of the measurement technique, but more a result of the diffraction produced by the edges of the samples that enhances absorption.

Questions

7.1 A sample of normal specific acoustic impedance ratio $z'_n = 2 - 6j$ at 200 Hz is placed in an impedance tube. At this frequency, the sound pressure level at a distance of 300 mm from the sample is 96 dB. Determine the complex amplitudes of the incident and reflected plane waves.

7.2 A 200 Hz plane wave is attenuated by 40 dB when travelling 1 m within an air-saturated porous material. The structure factor and porosity of the material are 1.5 and 0.95, respectively. Estimate the flow resistance of the material using the approximate expression in Eq. (7.11). You may assume an adiabatic fluid bulk modulus.

7.3 Solve Eq. (7.9a) for k' exactly in terms of s, ω, h, ρ_0 and K. Compare with the approximate solution given by Eqs (7.11) and (7.12) in the case $s = 1.5$, $h = 0.95$, $\sigma = 5000\ \text{kg m}^{-3}\ \text{s}^{-1}$ and $K = 1.0$ at 200 Hz. Substitute the approximate solution for σ obtained for the answer to the previous question and re-estimate the attenuation in dB per metre.

7.4 From Eq. (7.10) calculate z_c for $h = 0.95$, $K = 0.90$, $s = 1.5$, $\sigma = 10^4\ \text{kg m}^{-3}\ \text{s}^{-1}$ at 100 Hz and 1 kHz, assuming that the material is saturated with air. Compare with the approximate value based upon Eq. (7.13).

7.5 A cloth having a flow resistance of $1000\ \text{kg m}^{-2}\ \text{s}^{-1}$ is placed over a sheet of porous foam of which $z'_n = 1.6 - j10^3/f$. Calculate the normal incidence absorption coefficient at 100 Hz and 1 kHz.

7.6 A sound absorber comprises a 2-mm thick perforated aluminium sheet covering a thick sheet of mineral wool. The holes in the perforate are 3 mm in diameter and arranged in square array at a pitch of 12 mm. The resistance of the perforate is $50\ \text{kg m}^{-2}\ \text{s}^{-1}$. The normal specific acoustic impedance ratio of the mineral wool surface at 1 kHz is $1.6 - 0.5j$. Calculate the normal incidence absorption coefficient of the absorber at 1 kHz. Also calculate the mass per unit area equivalent to the inertial impedance of the perforate. [Hint: See the penultimate paragraph of Section 4.4.1.]

7.7 Confirm Eq. (7.25) by double differentiation of $\alpha(\phi)$ with respect to ϕ.

7.8 A limp porous sheet has a resistance ratio $R' = 2.0$ and mass per unit area m. Calculate the sound power dissipation coefficient at an angle of incidence of 45° and frequencies of 200 Hz and 2 kHz for values of m of 1.0 and 0.1 kg m^{-2}. The porosity may be taken as unity.

7.9 The same material is placed parallel to a rigid wall at a distance of 250 mm. Calculate the absorption coefficient at 45° at a frequency such that $kl = (\pi/2)\sec\phi$. [Hint: Eq. (7.48).]

7.10 The reverberation time of an empty room in the 500 Hz 1/3 octave band is 5.5 s. Its volume is 350 m^3 and its surface area is 300 m^2. With a 10 m^2 sheet of material placed on the floor, the reverberation time is 4.2 s. Estimate the diffuse field absorption coefficient of the sample.

8
Sound in Waveguides

8.1 Introduction

In previous chapters we have considered the generation and propagation of sound in volumes of fluid in which no single direction of propagation was preferred or special: sound energy could spread without limit. However, within ducts, which are ubiquitous components of manufacturing and process plant, power generation plant, gas, oil and water distribution networks and heating and ventilation systems, sound energy is constrained to follow their particular routes. Flow-generating devices, flow-control devices and turbulent flow all generate sound in ducts. If allowed to escape, it can have adverse effects on the health of personnel, on the surrounding environment and on verbal and musical communication in auditoria, lecture rooms and schools. The radiation of sound from the compressors and bypass fans of jet aircraft, and from the exhaust stacks of electrical power-generating gas turbines, is dependent upon the coupling of the sources to the acoustic modes of the ducts that contain them, and on the coupling of these modes to the outside air. Noise generated internally if sufficiently intense, threatens the mechanical integrity of duct structures, and has been known to produce fatigue damage of walls and even valve failure. Noise generation within ducts does have its positive aspects; for example, water pipe leak detection is based upon time taken for sound to travel from leaks to transducers placed in various positions along a pipe. The modelling, analysis and measurement of sound in ducted fluid systems are clearly of great importance in engineering acoustics.

Sound waves generated in a duct are continuously reflected by the walls so that the sound is guided along its path; hence a duct is said to form an acoustic 'waveguide'. There are two principal effects of this confinement: it limits the spatial forms of sound field that may propagate sound energy at any particular frequency; and it suppresses the geometric attenuation of sound which occurs in free field, so that the sound power flux in a duct of uniform cross-section is independent of position, except in as much as it may be attenuated by dissipative mechanisms. In practice, most ducts are not entirely uniform but incorporate features such as bends, junctions, area transitions and branches. Many also incorporate flow-control devices such as valves, dampers and diffusers; these reflect and scatter sound so that the resulting fields are very complex. In a textbook on fundamentals, it is not possible to deal with the great diversity of geometric forms of duct that are encountered in practice, or with the complicating influences of mean flow, turbulence and non-uniform temperature. Consequently, the analytical section of the chapter is confined to sound propagation in uniform ducts, and networks thereof, containing otherwise stationary fluid. The term 'duct' may be taken to include all pipes, tubes, conduits and closed channels.

Sound fields in uniform ducts fall into two broad categories. At frequencies where the acoustic wavelength considerably exceeds the peripheral length of a duct cross-section, the only form of sound field that can propagate freely, and can transport sound energy, is the axial plane wave. Other, non-planar, field components are created by sources of sound, and by geometric non-uniformities within ducts; but these decay rapidly with axial distance from the source. Sound fields in small-diameter pipes and tubes, such as domestic gas, oil and water pipes, hydraulic lines, and car exhaust pipes fall into this category over most of the audio-frequency range. Such ducts may be modelled as one-dimensional 'transmission lines' that may be connected to form networks. This form of model is used in Sections 8.2–8.6.

At frequencies where the acoustic wavelength is of the order of the cross-section peripheral length, or less, interference between wall reflections produces non-plane propagating forms of sound field that are characteristic of the shape of the duct cross-section; these are termed 'acoustic duct modes'. The higher the frequency, the greater the number of modes that are able to propagate. The sound power is shared among the propagating modes to a degree determined by the particular source. In practice, the plane wave mode tends to transport the major proportion of the power, except in ducts excited by high-speed rotating sources such as gas turbine rotors.

The transmission of sound energy along ducts can be inhibited by two forms of passive attenuator (we here exclude active control by means of loudspeakers). The insertion into a duct of cross-sectional areas S of a device or component that presents to a plane wave an acoustic impedance different from $\rho_0 c/S$ will create a reflected wave and therefore reduce the on-going proportion of *incident* sound power (although the *net* sound power will be the same on both sides if the device has a purely reactive effect). This mechanism of *reactive* attenuation is employed at low frequencies in the range where only plane waves propagate. At higher frequencies, reactive attenuation is less effective, and the resistive mechanism of sound absorption is employed. Various forms of porous material and acoustic resonators are introduced into a duct in such a way as to maximize the attenuation, and, in cases where fluid mass is transported, to minimize the resulting loss of static pressure (or flow energy).

The sound power radiated by a source into a duct is influenced by the presence of the duct walls. The pressure generated by a category of source that displaces fluid, such as an oscillating piston sliding in a tube, or a loudspeaker located in a duct wall, is greatly affected by the constraint on fluid motion applied by the walls. The impedance presented to the source is very different from that which is presented to the same source operating in free space, or in a plane baffle that bounds an otherwise unbounded fluid volume. Dipole source radiation is altered by the presence of duct walls because reflection effectively produces source images, which may increase or reduce the radiated power, depending upon the orientation of the dipole relative to the wall.

Particularly strong, frequency-dependent, variations of impedance are presented to a source by reflections of sound from impedance discontinuities in a duct. For example, the impedance presented to a source of unsteady mass introduction, such as the flow of internal combustion (I.C.) engine exhaust gas into an exhaust manifold/pipe, is dependent upon the reflections created by reactive attenuators downstream, and also the reflection from the open end of the pipe. These impedance variations cause the sound power generated by such Category 1 sources to vary in concert. The sound power generated by Category 2 sources, such as the axial momentum fluctuations generated by

compressor blades, is affected by the influence of duct reflections on the associated volume velocities.

This dependence of sound power on the acoustical properties of the duct complicates the analysis of the effect of attenuators inserted into a duct for the purpose of noise control. It is possible for an insertion to produce an increase in sound power generated by an in-duct source that may exceed the attenuation produced by the attenuator, thereby producing a net *increase* in the sound power transmitted by the system. This has significant implications for the design of standardized procedures for evaluating the sound power of ducted sources such as ventilation fans. Acoustic resonances of a duct can dramatically affect the behaviour of aeroacoustic sources such as oscillatory boundary layer separation and associated vortices produced by flow over solid bodies within the duct. Such a flow–acoustic interaction mechanism has led to serious vibration and damage to the heat exchangers of power-generation plant. On a more positive note, the operation of wind instruments such as clarinets and pipe organs depends crucially upon this form of interaction.

This chapter begins with a descriptive account of the behaviour in the time domain of plane wave pulses generated by impulsive piston displacement in a uniform tube that has various forms of termination. Subsequent analysis in the frequency domain of plane wave fields in simple acoustic transmission lines of uniform cross-section terminated by various forms of impedance illustrates the phenomena of characteristic (natural) frequencies, characteristic functions (modes) and resonance. The vibroacoustic interaction between a piston and a fluid in a tube is analysed in order to illustrate coupled fluid–structure modes and resonance. The application of acoustic impedance to the modelling of transmission line networks is then introduced, together with some archetypal examples of predominantly reactive attenuation systems.

The chapter continues with an analysis of sound propagation in a uniform two-dimensional waveguide with rigid walls. The phenomena of transverse modes and their associated cut-off frequencies are explained, together with modal phase and group velocity. The rigid walls are then replaced by locally reactive impedance boundaries that, if they have a resistive component, attenuate waves propagating in the duct. This is a simple model of a duct lined with sound-absorbent material. Modes of three-dimensional ducts of rectangular and circular cross-section are then briefly described, and modal excitation and energy flux in the former are examined. This section closes with examples of the attenuation performance of lined ducts and splitter silencers.

The final part of the chapter deals briefly with acoustic horns. The physical principle underlying their function is explained, the most simple form of the 'horn (wave) equation' is introduced, and the characteristics of some simple forms of horn are illustrated.

8.2 Plane wave pulses in a uniform tube

Figure 8.1 illustrates a uniform rigid-walled tube of cross-sectional area S fitted with a close-fitting, sliding, rigid piston at $x = 0$ and containing a fluid that is assumed to be inviscid. The tube is terminated by a rigid plug at $x = L$. At time $t = 0$, the piston is displaced very rapidly a very small distance into the tube and then rapidly brought to a halt (Fig. 8.1(b)). As shown by Fig. 8.2(a), a plane pulse of positive particle velocity travels away from the piston at speed of sound, accompanied by a plane pulse of positive

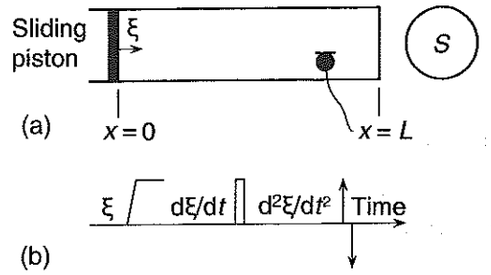

Fig. 8.1 (a) Piston-driven tube. (b) Displacement velocity and acceleration time-histories of the piston.

pressure in accordance with Eq. (3.29(a)). (Note: non-plane pulses cannot be generated by a uniformly moving rigid piston.) Work done by the piston on the fluid is transferred into energy transported by the pulse. After time $t = L/c$ the pulse reaches the rigid terminal plug, and a reflected pulse of equal and opposite particle velocity is generated by the requirement for the total particle velocity at the plug to be zero. In accordance with Eq. (3.29(b)), the reflected pulse pressure has the same magnitude and sign as the incident pulse. The reflected pulse travels back to the piston in time L/c. This pulse reflects off the now stationary piston to send a pulse identical to the original outgoing pulse down the tube, the process continuing indefinitely *if dissipative processes are absent*. The period of a signal from microphone installed flush with the tube wall is $2L/c$, which will produce a line spectrum with components at a harmonic series of frequencies given by $f_n = nc/2L$. These are the acoustic natural (characteristic) frequencies of a rigidly bounded fluid column of length L (see Section 8.3). (Will the spectrum vary with microphone position?) Following the cessation of activity of any form of source, *free* (unexcited) sound in the tube can exist *only at the natural frequencies*. The pulse pattern is illustrated in Fig. 8.2(b).

Suppose now that, instead of remaining stationary after its initial movement, the piston is rapidly returned to its original position at the instant when the reflected pulse hits it. In 'riding the punch' of the pulse, positive work is done by the fluid on the piston, the piston absorbs all its energy and the fluid returns to its original state of equilibrium. This is an elementary example of the general problem of the scattering of incident sound by a mobile body. The total scattered field is the sum of that scattered from the *motionless* body plus that *radiated* by any associated motion of the body. An immobile piston would generate a positive-going pulse of positive pressure, as in the preceding case; but the reverse motion of the piston produces a positive-going pulse of negative pressure, which cancels it. By a similar process, a loudspeaker can be made to absorb incident harmonic sound by driving it with an appropriate amplitude and phase.

If the piston is returned rapidly to its original position at the time when the original pulse hits the rigid termination (at time $t = L/c$), it will send a pulse of negative pressure and particle velocity down the tube (Fig. 8.2(c)). If the piston is then again displaced positively into the tube as the reflection of the original pulse hits it (at time $2L/c$) it will generate another positive pulse that, according to the principle of scattering explained above, will add to the reflection of the returning pulse from the piston as if stationary. If this process of periodic positive and negative piston displacement continues, the positive-going and negative-going pulses will be progressively amplified without limit:

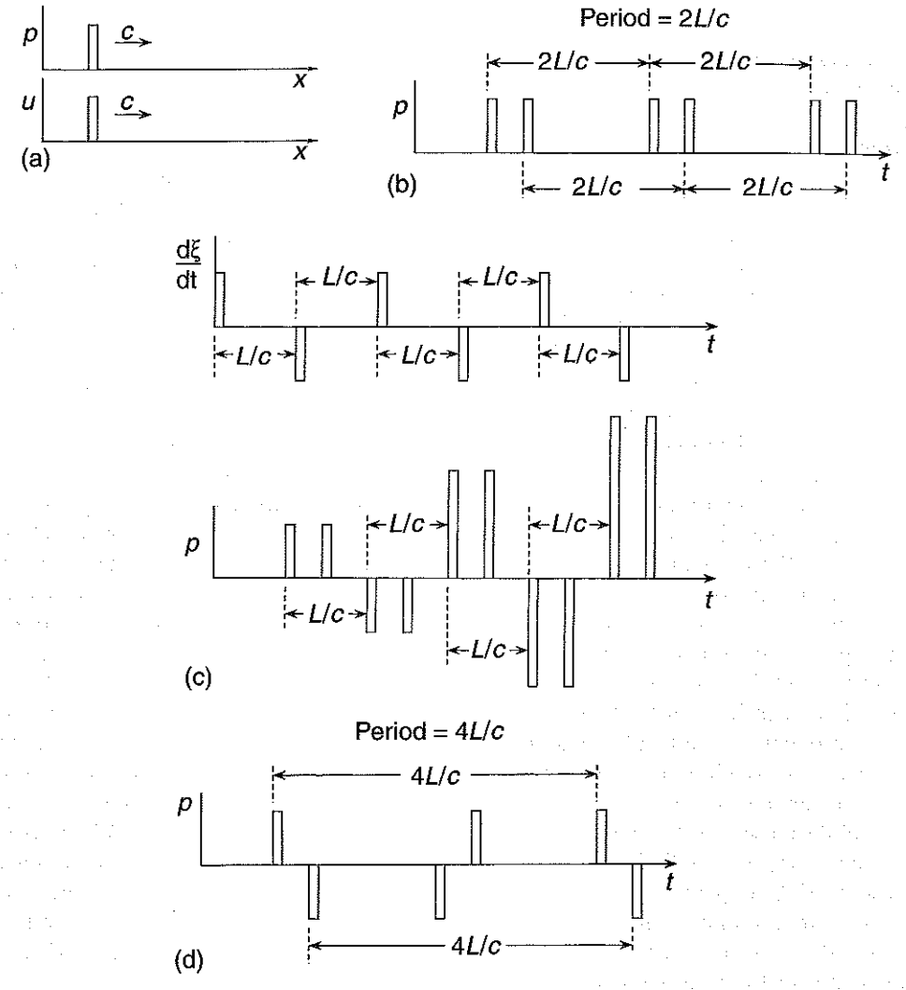

Fig. 8.2 (a) Pressure and particle velocity of the initial pulse. (b) Free pulse pattern. (c) Pulse pattern with cycled piston. (d) Free pulse pattern in a tube with pressure-release termination.

acoustic *resonance* is occurring at *all* the natural frequencies of the tube. The energy of the acoustic field grows as the square of the number of passages of the reflections. Note that the amplitude spectrum of the pulse patterns detected by a microphone depends upon its location because the spacing between the positive- and negative-going pulses varies with position. (Students are encouraged to verify this statement.)

If the fundamental period of piston displacement does not coincide with the inverse of any of the natural frequencies, resonance, and the associated progressive amplification of the acoustic pulses, do not occur. The total number of pulses in the tube grows with time but, because they do not superimpose, the acoustic energy increases only linearly with the number of passages of the reflections. We see that sound can be *excited* in the tube at *any frequency* but that resonance only occurs if the excitation has frequency components that coincide with one or more natural frequencies.

Suppose now that the rigid plug termination is removed to produce an open-ended tube and that the piston is given a single positive impulsive displacement. The radiation resistance ratio of an open tube end at low frequencies ($ka \ll 1$) is half of that of a rigid piston oscillating in a baffle (Eq. (6.55)), and the additional freedom for the near field to 'wrap around' the end of the pipe in the absence of a baffle reduces the reactive component from $8\,ka/3\pi$ to $0.6\,ka$, where a is the tube radius. The impedance ratio in this frequency range is so small that we may initially assume for the purpose of the present exercise that, together with the pressure, it is zero (the so-called 'pressure-release' condition). In this case, an initial pulse of positive pressure is reflected as one of equal negative pressure; the particle velocities in both incident and reflected pulse are therefore equal and both *positive* (Fig. 8.2(d)). This negative pulse is then reflected by the now stationary piston as a negative pulse, which is subsequently reflected at the open end as a positive pulse, which then returns to the piston. The pulse has traversed a distance of $4L$ during one cycle. The sequence is now repeated endlessly.

In this case, the fundamental period of the pressure pulse train resulting from a single initial displacement of the piston is equal to $4L/c$. This corresponds to a fundamental natural frequency that is one half of that of the rigidly terminated tube. If the piston is pulsed at twice this rate, alternate pulses are cancelled at the piston surface, which shows that twice the fundamental frequency is not a natural, or resonance, frequency of this system, in contrast to the closed tube. Pulse sequence analysis demonstrates that the natural (and resonance) frequencies of the open-ended tube are restricted to *odd* multiples of the fundamental frequency, given by $f_n = (2n - 1)c/4L$.

In fact, a tube opening has a small positive reactance. This has the effect of making it slightly longer, in acoustical terms, than the geometric length. The 'end correction' to L for the opening of an unflanged circular section tube is approximately 0.6 times the radius a, so reducing the natural frequencies. Low frequency radiation resistance is such that the low-frequency sound energy is weakly radiated by each incident pulse, so that it slowly decreases, unless the piston is periodically displaced to inject new energy. If so, resonant response is limited by the requirement for input power to balance radiated power. High-frequency energy is radiated very effectively upon its first encounter with the opening, so that no high-frequency resonance is possible. This form of behaviour, in which the stronger resonances are confined to the lower harmonics, is characteristic of many musical wind instruments.

We now suppose that the tube is terminated by a device that offers a purely *resistive* impedance having a specific acoustic resistance ratio denoted by r. It can be closely realized by placing a rigid porous sheet over the open end of a tube. In the $ka \ll 1$ frequency range, r can be selected to be far greater than both the real and imaginary parts of the radiation impedance with which it is in series. The piston is given a rapid positive displacement, as before. The pulse is reflected from the termination (unless $r = 0$); but now the form of the reflection depends upon whether r is greater or less than unity. The ratio of pressure amplitudes of reflected to incident waves is given by Eq. (7.20) as

$$R = (r - 1)/(r + 1) \tag{8.1}$$

If $r > 1$, the pressure of the reflected pulse at the termination is positive and the associated particle velocity is negative. The piston is given a negative displacement at the time the initial pulse hits the termination, generating a pulse of negative acoustic pressure and particle velocity. It is then given a positive displacement at the time when

the reflection of the initial pulse hits it. The particle velocity of the pulse that it generates will be equal to the sum of that which it would produce in the absence of the reflection (i.e. that of the original pulse) *plus* that produced by the reflection of the returning pulse from its surface as if stationary. Hence the positive pressure of the new pulse will be in the ratio $2r/(1 + r)$ to that of the original pulse. The process is then repeated, the next pulse produced by positive piston displacement being in the ratio $3r^2 + 1/(1 + r)^2$ to the original pulse. The same progression will apply to the pulses produced by the negative displacement of the piston. The reader is left to continue the progression, whereupon it will be found that the ratio will asymptote to a finite value that increases with r; with $r = 2$, the asymptotic value of the ratio is 1.5. Resonances occur, but the energy in the tube remains finite because the resistive termination dissipates energy. A similar exercise may be carried out for values of r less than unity; again the energy in the tube remains finite.

It should be noted that the resonance frequencies are the same with a rigid plug as with a termination having $r > 1$; and they are the same as for the open end of negligible impedance with $r < 1$. This is because a resistance of the termination is assumed not to be frequency dependent and imposes no time delay on the reflection. However, reactive terminations in the form of an acoustic 'spring' (such as the air within a layer of porous foam at low frequency), or acoustic 'mass' (such as that associated with a perforated sheet) do introduce time shifts because the particle velocity induced by a pressure acting on the termination is proportional to the time derivative and time integral of the pressure, respectively. In frequency domain terms, these forms of termination induce phase shifts of the $\pm\pi/2$ on the reflected waves. They therefore alter the natural and resonance frequencies from those with a purely resistive termination.

8.3 Plane wave modes and natural frequencies of fluid in uniform waveguides

In the previous section, some aspects of one-dimensional waveguide behaviour in the frequency domain have been inferred from pulse train patterns in the time domain. We now develop a more rigorous analysis of the plane wave modes and natural frequencies by solving the Helmholtz equation (Eq. (3.20)) subject to the boundary conditions imposed by the terminations. The practical importance of the following models is not limited to their applications to acoustic transmission lines. Uniform ducts carrying plane waves constitute one-dimensional enclosures. Study of their natural frequencies, modes, response to excitation and energy flow behaviour prepares the ground for the subsequent analysis and physical understanding of the behaviour of sound in two- and three-dimensional ducts, and for extension in the following chapter to the acoustics of three-dimensional enclosures, which is of vital importance to the field of internal vehicle noise. The following section also presents a case of fluid–structure interaction, which is an elementary example of a type of problem commonly encountered in the field of vibroacoustics. We begin by assuming that the terminations are conservative and do not absorb (dissipate) sound energy.

8.3.1 Conservative terminations

If the impedance of a termination is purely imaginary (reactive), it absorbs no energy

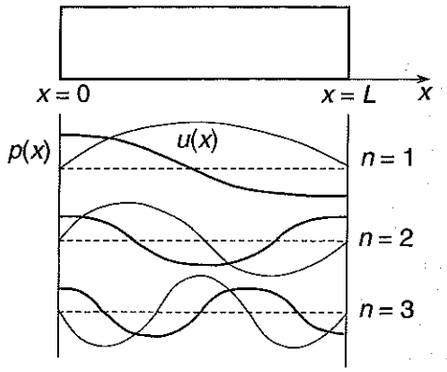

Fig. 8.3 Pressure and particle velocity distributions of low-order standing waves in a closed tube.

from the fluid. Consider first the case shown in Fig. 8.3 of rigid terminations at $x = 0$ and $x = L$. Equation (3.23) gives the general harmonic solution for pressure in the form

$$p(x, t) = [\tilde{A} \exp(-jkx) + \tilde{B}(jkx)] \exp(j\omega t) \tag{8.2}$$

The particle velocity is zero at $x = 0$. Equation (3.31) gives $\tilde{A} = \tilde{B}$. The spatial distributions of sound pressure and particle velocity are given by

$$p(x, t) = 2\tilde{A} \cos kx \exp(j\omega t) \tag{8.3}$$

and

$$u(x, t) = (j/\omega\rho_0)\partial p/\partial x = -(2j\tilde{A}/\rho_0 c) \sin kx \exp(j\omega t) \tag{8.4}$$

The zero particle velocity condition at $x = L$ can only be satisfied if $\sin kL = 0$ or $kL = n\pi$: the tube length equals even integer multiples of half a wavelength. The only allowed frequencies of *free* vibration are thus given by

$$f_n = nc/2L \tag{8.5}$$

This result confirms the conclusion from the pulse model presented above.

These special frequencies are termed 'natural' or 'characteristic' frequencies because they are proper to the system. Mathematicians also call them 'eigenfrequencies' from the German word 'eigen', which means 'own'. These correspond to the harmonics of the velocity–time history of the periodically pulsed piston in the case of rigid termination illustrated in Fig. 8.2(c). The corresponding spatial distributions of sound pressure are given by

$$p(x) = 2\tilde{A} \cos(n\pi x/L) \tag{8.6}$$

as illustrated by Fig. 8.3. Note that these pure standing waves may be termed 'characteristic functions' or 'eigenfunctions'. Engineers more commonly called them 'modes' (meaning 'forms'). These modes form an 'orthonormal set' in that they satisfy the condition of orthogonality; in the case of a uniform medium, this means that the integral of the product of any two different eigenfunctions over the bounded domain is zero. Each mode therefore behaves like an *independent* single-degree-of-freedom oscillator. The total energy is the sum of the modal energies, irrespective of their

respective amplitudes. The complex amplitude $2\tilde{A}$ is undetermined, because no excitation has been assumed to exist.

Now we assume that the impedance of the termination at $x = L$ is zero. Equation (8.3) requires $\cos kL$ to equal zero. Hence the natural frequencies are given by $kL = (2n - 1)\pi/2$ or $f_n = (2n - 1)c/4L$. In this case, $L = (2n - 1)\lambda/4$; that is, odd integer multiples of $\lambda/4$, confirming the conclusions from the pulse study above. The corresponding modes take the form $p(x) = 2\tilde{A} \cos[(2n - 1)\pi x/2L]$. These modes form an orthonormal set.

As a further example, we now assume a termination that is purely inertial in nature, having a specific acoustic impedance ratio given by $z'_t = j\omega m/\rho_0 c$, where m represents mass per unit area. Equations (8.3) and (8.4) give the specific acoustic impedance ratio at position x in the field as

$$z'(x) = j \cot kx \tag{8.7}$$

which must equal that of the termination at $x = L$. Hence,

$$\cot kL = \omega m/\rho_0 c = (kL)(m/\rho_0 L) \tag{8.8}$$

The solutions for kL correspond to the natural frequencies of the system that are represented by the intersections of the curves presented in Fig. 8.4(a). The presence of the inertial termination is seen to *increase* the natural frequencies relative to those with the rigid termination, the ratio tending towards unity as frequency – and impedance – increases. With a very large mass, the lowest natural frequency corresponds closely with that of the mass coupled to a spring whose stiffness equals that produced by bulk compression of the whole volume of fluid. With very small inertial impedance the natural frequencies tend to those of a tube open at one end. Figure 8.4(a) shows that the natural frequencies do not form a harmonic series. The wavenumbers corresponding to the natural frequencies are greater than for the rigidly closed tube, and therefore the associated wavelengths are shorter.

In the case of a purely elastic termination of stiffness per unit area s at $x = L$, the term $-(sL/\rho_0 c^2)/kL$ replaces the inertial term on the right-hand side of Eq. (8.8). The solutions for natural frequencies correspond to the intersections shown in Fig. 8.4(b). The frequencies do not form a harmonic series. The presence of the elastic termination is seen to *decrease* the natural frequencies relative to those of the rigidly closed tube, the ratio increasing as frequency increases. For very small elastic impedances the natural frequencies tend to those of an open tube, and for very large elastic impedance they tend to those of a tube with rigid termination.

The acoustic modes of fluid systems having finite, reactive impedance boundaries, such as the two above, do not form orthonormal sets, although the complete system, including the boundary structures, does satisfy a more general form of orthogonality condition that is beyond the scope of this book.

The natural frequencies of the system with a termination consisting of an *undamped* mass–spring oscillator are easily found from the construction of Fig. 8.4(c). At its *in vacuo* natural frequency ω_0, the impedance of the oscillator is zero, but this will not be a natural frequency of the system unless $k_0 L = \omega_0 L/c$ also equals $(2n - 1)\pi/2$. This system is an elementary case of fluid–structure coupling in which the dynamic properties of both media influence the coupled natural frequencies and modes.

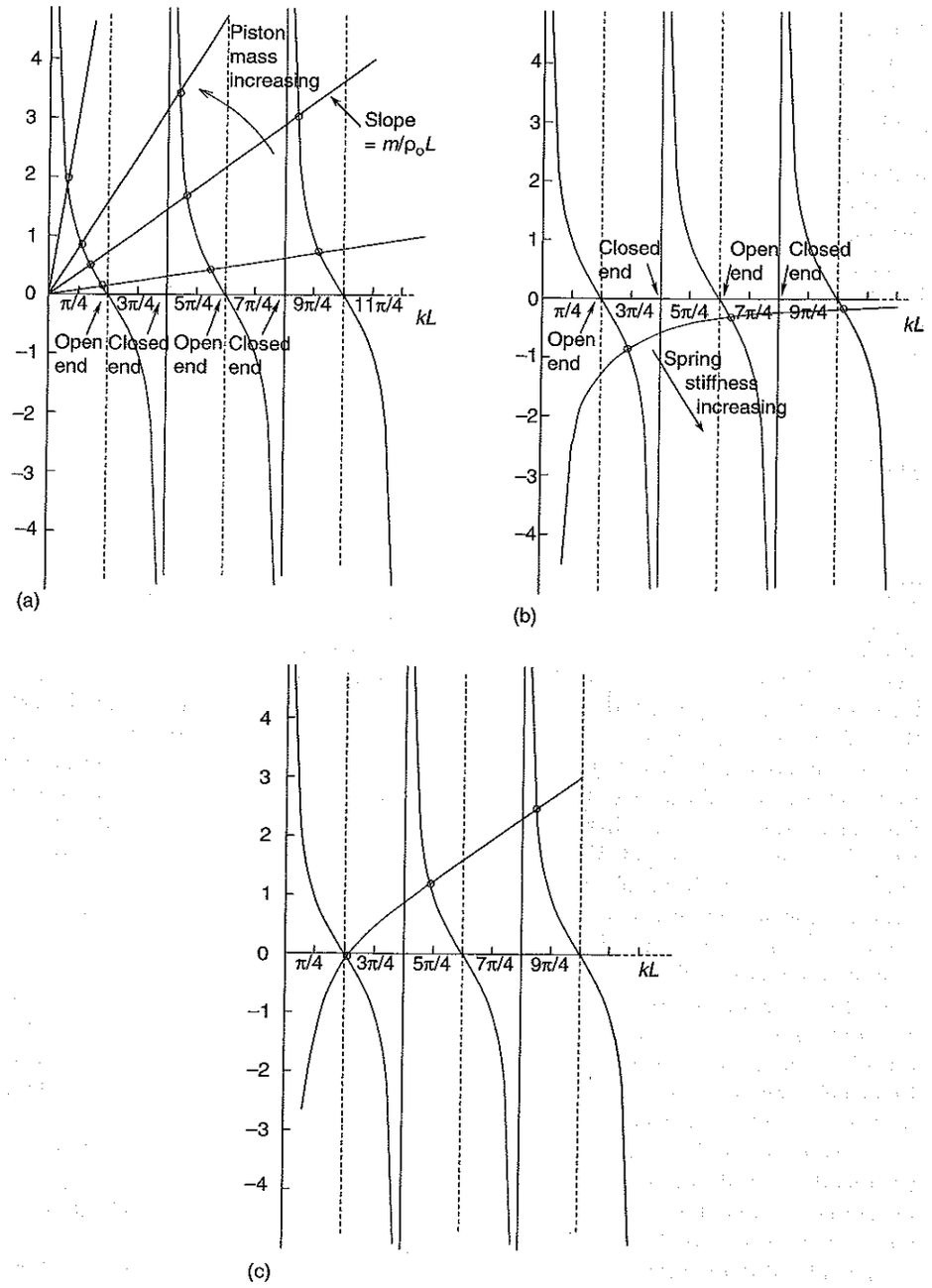

Fig. 8.4 Intersection of acoustic and mechanical impedance curves indicate natural frequencies of a tube terminated by: (a) a lumped mass; (b) an elastic spring; (c) an earthed mass–spring system.

8.3.2 Non-conservative terminations

Consider the model of a tube terminated rigidly at $x = 0$ and at $x = L$ by a frequency-independent complex impedance having non-zero resistance. The dissipation of sound energy by a resistive termination must be reflected in the form of the time dependence of pressure and particle velocity in *free* vibration. Unless a termination is perfectly absorbent (anechoic), sound energy will be stored in the interference field, which exhibits quasi-periodicity produced by multiple reflection of travelling waves at the boundaries. (A free oscillatory field losing energy cannot be perfectly periodic since it never exactly repeats any specific state.) The rate of energy leakage will be equal to the energy flux, or intensity, of the field. Intensity is equal to the product of pressure and particle velocity. Energy is proportional to the square of particle velocity or pressure, which are linearly related to each other. Hence, the rate of energy loss will be proportional to the stored energy. Consequently, energy varies exponentially with time, and pressure and particle velocity decrease exponentially at half the rate of energy.

We may therefore express the combination of quasi-periodicity and exponential decay by assuming a time dependence in the form $\exp(j\omega t)\exp(-\delta t)$. The exponent may equivalently be written as a function of a complex frequency in the form $\exp(j\omega' t)$, where $\omega' = \omega + j\delta$. In the exponential representation, the locus of the associated phasor takes the form of a spiral instead of the usual circle. Readers may be uneasy with this concept, but it is compatible with the expression for the free vibration of a viscously damped oscillator developed in Appendix 5.

(Note: since complex frequency does not represent pure harmonic motion, we may not strictly employ the concept of impedance at real frequency ω in the following analysis. However, provided that the fractional decrease in amplitude over *one cycle of oscillation* is very much smaller than unity ($2\pi\delta/\omega \ll 1$), the bandwidth of the spectrum is so small as to allow us to use impedance at frequency ω with insignificant error. This condition also ensures that the damping of any mode is very much less than the critical value.)

We may now introduce the complex frequency into the wave equation and seek a solution for the associated spatial distribution of the sound pressure and particle velocity. We assume an expression for the sound pressure in the form $p(x, t) = \tilde{A}\exp(\lambda x)\exp(j\omega' t)$ and introduce it into the wave equation to give

$$[\lambda^2 + (\omega'/c)^2]\tilde{p} = 0 \tag{8.9}$$

The solutions for λ are

$$\lambda = \pm j(\omega'/c) = \pm jk' \tag{8.10}$$

where $k' = k + j\delta/c$ is a complex wavenumber, a concept previously encountered in Chapter 7. However, there is a crucial difference between the significance of the imaginary part of the wavenumber in the two cases.

The complexity of the wavenumber in Eq. (7.7), which expresses the spatial distribution of pressure in waves travelling in resistive media, arises from the continuous loss of sound energy to heat as the waves propagate; this accounts for its negative imaginary part ($-j\alpha$). In the present case, the fluid medium is assumed to be inviscid, and no such propagation loss occurs. The complexity of k' here arises from the assumption of exponential temporal decay. The imaginary part of k' is positive, seemingly expressing an exponential growth with distance travelled by each plane travelling wave. However,

neither of these two *individual* waves is a complete solution to the homogeneous wave equation in a bounded volume. We shall find that their combination in the form of an interference field exhibits no non-physical amplification and no energy dissipation within the fluid. Energy is simply transported towards the resistive termination by means of progressively weaker spatial oscillations of energy.

The pressure field takes the general form

$$p(x, t) = [\tilde{A} \exp(-jk'x) + B \exp(jk'x)] \exp(j\omega' t) \tag{8.11}$$

The particle velocities in the right- and left-travelling waves are given by the momentum equation as

$$u^+(x, t) = (j/\omega'\rho_0)\, \partial p^+/\partial x = (\tilde{A}/\rho_0 c) \exp(-jk'x) \exp(j\omega' t) \tag{8.12a}$$

or

$$u^+(x, t) = p^+(x, t)/\rho_0 c \tag{8.12b}$$

and

$$u^- = (j/\omega'\rho_0)\, \partial p^-/\partial x = -(\tilde{B}/\rho_0 c) \exp(jk'x) \exp(j\omega' t) \tag{8.13a}$$

or

$$u^-(x, t) = -p^-(x, t)/\rho_0 c \tag{8.13b}$$

The pressures and particle velocities are, as expected, related by the characteristic acoustic impedance of a lossless fluid, unlike that of Eq. (7.10).

The rigid boundary condition at $x = 0$ requires that $\tilde{A} = \tilde{B}$. Hence the pressure field is expressed as

$$p(x, t) = 2\tilde{A}[\cos(kx) \cosh(\delta x/c) - j \sin(kx) \sinh(\delta x/c)] \exp(j\omega' t) \tag{8.14}$$

the particle velocity field is expressed as

$$u(x, t) = (2\tilde{A}/\rho_0 c)\, [\cos(kx) \sinh(\delta x/c) - j \sin(kx) \cosh(\delta x/c)] \exp(j\omega' t) \tag{8.15}$$

The specific acoustic impedance ratio at position x is given by

$$z'(x) = p(x)/\rho_0 c\, u(x) = j \cot k'x \tag{8.16}$$

of which the phase is $\phi_{pu} = \tan^{-1}[\sin(2kx)/\sinh(2\delta x/c)]$. This differs from the pure standing wave value of $\pm\pi/2$, and varies with x.

Solutions for the complex natural frequencies and mode shapes of the system are found by equating the expression in Eq. (8.16) with $x = L$ to the specific impedance ratio of the termination z'_t. Thus

$$\cot k'L = -jz'_t \tag{8.17}$$

Since we are concerned here with the non-conservative action of a termination, we shall restrict z'_t to a purely resistive component r. (Note: the prime is omitted in the following analysis for the sake of typographical simplicity.) This will considerably simplify the analysis and its physical interpretation. Equation (8.17) now becomes

$$\cos k'L = -jr \tag{8.18}$$

This equation may be separated into real and imaginary parts to give

$$\exp(2\delta L/c) \cos(2kL) = (r + 1)/(r - 1) \tag{8.19a}$$

and

$$\exp(2\delta L/c) \sin(2kL) = 0 \tag{8.19b}$$

We distinguish two sets of solutions of Eq. (8.19b). When $r < 1$, $kL = n\pi/2$, with n odd; when $r > 1$, $kL = n\pi/2$ with n even. The first set of solutions for kL corresponds to the natural frequencies of a tube with zero impedance at one end and the second set corresponds to those of a rigidly terminated tube. This is in agreement with the conclusions from the foregoing pulse studies that purely resistive impedance introduces no time delay (or phase change) in the reflected pressure relative to the incident pressure. The solution of Eq. (8.19a) for $r > 1$ is

$$\delta L/c = \ln[(1 + r)/(r - 1)]^{1/2} \tag{8.20a}$$

which, for $r \gg 1$, is well approximated by

$$\delta \approx c/Lr \tag{8.20b}$$

For $r < 1$, the solution to Eq. (8.19a) is

$$\delta L/c = \ln[(1 + r)/(1 - r)]^{1/2} \tag{8.21a}$$

which, for $r \ll 1$, is well approximated by

$$\delta \approx cr/L \tag{8.21b}$$

The variations of δ with r clearly indicate the tendency for the modal damping to increase as r tends to 1, which corresponds to zero reflection and an absence of modal behaviour. The linear dependence of δ on c/L is physically reasonable: the rate of energy flow towards the termination is proportional to c and stored energy is proportional to L. The limit $2\pi\ \delta/\omega \ll 1$ proposed for valid use of impedance corresponds to $r \gg L/\lambda$ if $r > 1$ or $r \ll L/\lambda$ if $r < 1$. The resulting general expression for the pressure distribution in a natural mode is

$$p(x) = 2\tilde{A}[\cos(k_n x) \cosh(\delta x/c) - j \sin(k_n x) \sinh(\delta x/c)] \tag{8.22}$$

with k_n and δ/c appropriately chosen to suit the value of r. These are 'complex modes' in which the phase of the pressure varies continuously with x, unlike real modes in which the phase varies in steps of $\pm\pi/2$ at nodes. The phase of the modal pressure at x relative to that at $x = 0$ is

$$\phi(x) = \arctan[-\tan(kx) \tanh(\delta x/c)] \tag{8.23}$$

All bounded elastic systems with resistive boundaries possess complex natural modes. The physical reason is that in free decay from an initially excited state, the stored energy must leak towards the resistive boundaries. Analysis of the instantaneous intensity in the time domain is algebraically complicated and the details are omitted for the sake of brevity. It reveals that the physical process involves the 'pumping' of energy towards the termination by largely reactive oscillatory exchanges between locally stored kinetic and potential energy in the manner explained in Chapter 5; but with some cyclic 'leakage' of energy towards the resistive boundary associated with the fact that the energy 'swings' progressively weaken with time because of the time decay component inherent in complex frequency.

8.4 Response to harmonic excitation

8.4.1 Impedance model

It is generally much easier to find solutions for the response of dissipative systems to harmonic excitation than those for free vibration because energy is continuously injected to maintain pure harmonic motion. In principle, the impulse response of dissipative systems can be determined from the harmonic response by means of the inverse Fourier transform (see Appendix 4), but mathematical difficulties can arise if non-causal forms of dissipation, such as hysteretic damping, are assumed (see Appendix 5).

We assume that a piston sliding in a tube undergoes inexorable harmonic oscillation with velocity $u = \tilde{U}\exp(j\omega t)$. ('Inexorable' means that the impedance of the piston and its driving mechanism is so high that it maintains its amplitude irrespective of the reaction of the fluid in the tube. This is not the case with a real loudspeaker.) The specific acoustic impedance ratio presented to the piston at $x = 0$ is given by Eq. (4.22) as

$$z'(0) = \frac{z'_t + j\tan kL}{1 + jz'_t \tan kL} = \frac{r(1+\tan^2 kL) + j[x(1-\tan^2 kL) + (1-x^2-r^2)\tan kL]}{(1-x\tan kL)^2 + (r\tan kL)^2} \tag{8.24}$$

in which z'_t has been written as $r + jx$. This expression may be termed a 'transfer impedance' relation. It may be applied to a series of individual sections of duct connected through impedance discontinuities to determine the impedance of the chain. The imaginary part of $z'(0)$ is zero when $2\tan kL = [(1-x^2-r^2)/x] \pm [((1-x^2-r^2)/x)^2 + 4]^{1/2}$. The real part of $z'(0)$ is always positive.

The sound pressure is related to the piston velocity by

$$p(x,t) = [\rho_0 c\,\tilde{U}/(\cos kL + jz'_t \sin kL)]\,[z'_t \cos(k(x-L)) - j\sin(k(x-L))]\exp(j\omega t) \tag{8.25}$$

which exhibits the resonance behaviour previously inferred from the pulse studies performed in the previous section. (Students should confirm and interpret this result.)

At frequencies for which $\tan kL = 0$, $z'(0) = z'_t$, the length of the tube equals an integer number of half wavelengths and the system behaves as if the terminal impedance were applied directly to the piston. These are the natural frequencies of the tube when closed rigidly at both ends. At frequencies for which $\tan kL = \infty$, $z'(0) = (z'_t)^{-1}$, the length of the tube equals an odd number of one-quarter wavelengths and the specific acoustic impedance ratio presented to the piston is the *inverse* of that of the termination. These correspond to the natural frequencies of the tube with a rigid plug at one end and a 'pressure release' termination at the other.

If z'_t is purely resistive

$$z'(0) = [r(1+\tan^2 kL) + j\tan kL\,(1-r^2)]/[1 + (r\tan kL)^2] \tag{8.26}$$

which equals unity at any frequency if $r = 1$ (zero reflection by the termination). The resonance frequencies are given by $\mathrm{Im}\{z'(0)\} = 0$, of which the solution $r = 1$ corresponds to a pure travelling wave system and only the solutions $\tan kL = 0$, $r > 1$ and $\tan kL = \infty$, $r < 1$ are relevant to resonance. This is consistent with Eq. (8.19b). The variation of $z'(0)$ with kL with $r = 3$ and $x = 0$ is plotted in Fig. 8.5.

If z'_t is purely reactive

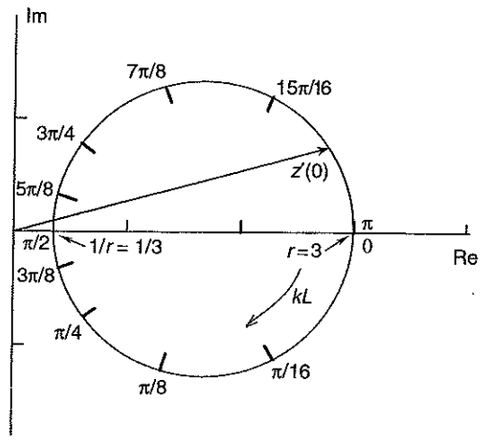

Fig. 8.5 Variation of $z'(0)$ presented to the piston with kL for $r = 3$ and $x = 0$.

$$z'(0) = j[x(1-\tan^2 kL) + (1-x^2\tan kL)]/[1-x\tan kL]^2 \tag{8.27}$$

which is purely imaginary at all frequencies. This makes physical sense because a purely reactive termination can dissipate no energy. The resonance frequencies are given by $\mathrm{Im}\{z'(0)\} = 0$, or $\cot kL = x$, which is consistent with Eq. (8.8).

The power radiated into the tube per unit cross-sectional area is given by

$$W' = \frac{1}{2}\rho_0 c|\tilde{U}|^2\left[\frac{r(1+\tan^2 kL)}{(1-x\tan kL)^2 + (r\tan kL)^2}\right] \tag{8.28}$$

which is plotted in non-dimensional form Fig. 8.6 for $r = 3$ and $x = 0$.

The sound power radiated from an open-ended tube is of interest in relation to internal combustion engine exhaust pipes. The acoustic radiation impedance ratio at the opening is a complicated function of ka, except in the range of frequency where $ka \ll 1$, when it takes the approximate form $Z'_{a,rad} \approx (ka)^2/4 + j\,0.6\,ka = R + jX$. The sound power input to a tail pipe per unit volume velocity per unit cross-sectional area (most of which is radiated to the environment) is given by $W'' = \frac{1}{2}\rho_0 c\,\mathrm{Re}\{Z'(0)\}$, where $Z'(0)$ is

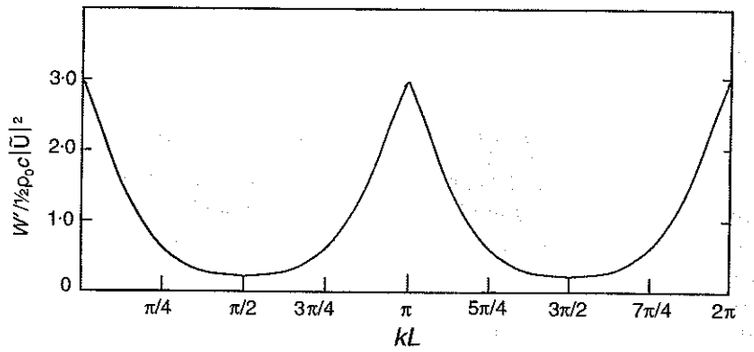

Fig. 8.6 Non-dimensional sound power radiated into the tube with $r = 3$ and $x = 0$.

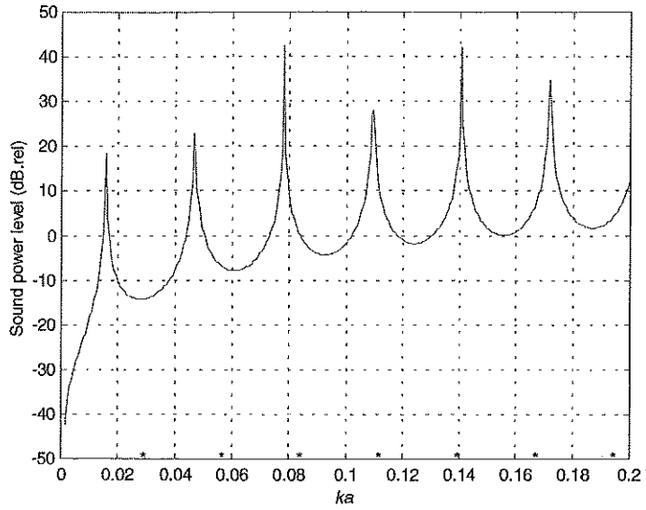

Fig. 8.7 Normalized sound power radiated into an exhaust tail pipe. $L/a = 100$; $c = 399$ m s^{-1}; $\rho_0 = 1.0$ kg m^{-3}.

given by Eq. (8.24) with $r + jx$ replaced by $R + jX$. The normalized sound power input to a tail pipe of length L is plotted in Fig. 8.7 for $L/a = 100$ up to $ka = 0.2$. The mean gas density has been taken as 1.0 kg m^{-3}. This corresponds to a frequency of 727 Hz for a 35-mm diameter exhaust pipe. Note that k in the exhaust pipe has been taken to be 0.86 times that in the outside air to allow for the elevated speed of sound in the exhaust gas. The effect of pipe resonances on the power is clearly seen. At frequencies for which $kL = (2n - 1)\pi/2$ or $ka = (2n - 1)\pi/200$, the inlet impedance ratio equals the inverse of the outlet impedance ratio, and is therefore large. A four-stroke engine running at 3000 rpm exhausts gas with harmonic frequency components at integer multiples of 100 Hz, which correspond to integer multiples of $ka = 0.0276$, as indicated on the figure. Clearly, some harmonics of the source can coincide with peaks in the radiated power curve as engine speed and/or exhaust gas temperature varies. This model is a gross approximation to the real physical system, partly because the impedance presented by an exhaust system to the exhaust valve opening can be sufficiently large at certain frequencies to affect the exhaust flow. Tuning of the system to optimize scavenging (discharging the exhaust gases) is therefore possible.

8.4.2 Harmonic response in terms of Green's functions

An alternative approach to developing expressions for the response of a fluid in an enclosure to boundary vibration is offered by the Kirchhoff–Helmholtz (K–H) integral equation (6.48). As explained in Chapter 6 (Section 6.4.5), the boundary pressure term may be eliminated by selecting a Green's function that satisfies the inhomogeneous Helmholtz (harmonic wave) equation having a delta function source on the right-hand side (Eq. (6.10)), together with the condition of *zero normal pressure gradient* on all boundaries. Happily, we have already found functions that satisfy these conditions for a uniform duct in which only plane waves exist; they are the eigenfunctions (modes)

expressed by Eq. (8.6). They are known as the 'rigid-wall' modes and they form what is known as a 'complete set' of orthogonal functions. This means that any physical quantity that is continuously distributed over the length of the enclosed length of fluid may be expressed as a sum of these functions, each with a coefficient to give the correct physical dimensions.

[Note: *the rigid-wall modes and associated eigenfrequencies must not be confused with the natural modes and frequencies of a fluid volume that has other than rigid boundaries.* They constitute a set of so-called 'basis functions' because they form a basis for constructing a series representation of an arbitrary function. Their utilitarian importance is that it is easy to determine them, either analytically (in cases of boundaries having regular geometry) or numerically, using finite or boundary element models, and that they can be used conveniently to express the coupling between flexible enclosure boundaries and the contained fluid, as we shall see later. They also approximate very closely to the natural modes and frequencies of real 'almost rigid-walled' enclosures such as reverberation rooms.]

In accordance with the above, a Green's function for the tube of cross-sectional area S, which represents the particular pressure response to a harmonic delta function source of unit strength, may be expressed as the sum of an infinite series of rigid-wall modes, thus:

$$G(x|x_0) = \sum_{n=0}^{\infty} A_n \cos(n\pi x/L) \tag{8.29}$$

Substitution into the inhomogeneous Helmholtz equation with a one-dimensional delta function source term gives

$$\partial^2 G/\partial x^2 + k^2 G = -\delta(x - x_0)/S \tag{8.30}$$

Multiplication by $\cos(m\pi x/L)$ and integration over the length L yields, by virtue of the orthogonality of the eigenfunctions and the property of the delta function (Eq. (6.7)),

$$(L/2)\,[k^2 - (n\pi/L)^2]\,A_n = -(1/S)\cos(n\pi x_0/L) \tag{8.31}$$

because all the terms having $m \neq n$ disappear and $\int_0^L \cos^2(n\pi x/L)\,\mathrm{d}x = L/2$. Substitution for A_n in Eq. (8.29) gives the Green's function as

$$G(x|x_0) = \frac{2}{SL}\sum_{n=0}^{\infty}\frac{\cos(n\pi x_0/L)\cos(n\pi x/L)}{k_n^2 - k^2} \tag{8.32}$$

where $k_n = n\pi/L$.

Note that the one-dimensional delta function must be used because a point source would produce non-plane field components. It corresponds physically to a pulsating plane diaphragm traversing the duct at $x = x_0$ and has dimensions of $[L]^{-1}$. It is divided by the cross-sectional area of the duct, because the source must represent volume velocity *per unit volume* to satisfy dimensional compatibility with the terms on the left-hand side of the equation. (Students should check this.) The Green's function is now introduced into the K–H equation (6.46). Non-zero normal pressure gradients exist at the surface of the piston and at the surface of a termination of arbitrary, non-infinite impedance where the pressure gradient and pressure are related to the specific acoustic impedance ratio by $\partial p/\partial x = (jk/z_t)p$. The K–H equation becomes

$$p(x) = \int_S G(\partial p/\partial n)\,\mathrm{d}S = \int_{S_1} G(x|0)(-jk\rho_0 c\tilde{U})\,\mathrm{d}S_1 + \int_{S_2} G(x|L)(jk\,p(L)/z'_t)\,\mathrm{d}S_2 \quad (8.33)$$

where S_1 and S_2 represent the surfaces of the piston and termination, respectively. Note that the normal points *into* the fluid volume and therefore $\partial p/\partial n = -\partial p/\partial x$ at $x = L$. As explained in Chapter 6, the volume velocity generated by the action of pressure on the finite impedance boundary at $x = L$ appears to constitute a source. However, it is not an active source of energy, but a passive boundary response that affects the field by its induced motion.

The Green's function given by Eq. (8.32) is introduced into Eq. (8.33) to give the complex amplitude of pressure at position x in the duct as

$$p(x) = -\frac{2jk\rho_0 c\tilde{U}}{L}\left[\sum_n \frac{\cos(n\pi x/L)}{k_n^2 - k^2} - \frac{p(L)}{z'_t}\sum_n \frac{(-1)^n \cos(n\pi x/L)}{k_n^2 - k^2}\right] \quad (8.34)$$

in which integration over the end boundaries is replaced by the products of the normal pressure gradients with the cross-sectional area, because the field is plane. The series representation is now used to express $p(x)$ and $p(L)$ as

$$p(x) = \sum_m A_m \cos(m\pi x/L) \quad \text{and} \quad p(L) = \sum_q A_q (-1)^q \quad (8.35a,b)$$

Substitution in Eq. (8.34), followed by multiplication by $\cos(l\pi x/L)$ and integration over the length of the tube, yields

$$A_n[k_n^2 - k^2] = \left(\frac{2jk}{L}\right)\left[\frac{1}{z'_t}\sum_q (-1)^{n+q} A_q - \rho_0 c\tilde{U}\right] \quad (8.36)$$

Remarkably, the series solution of Eq. (8.35a), with $A_m = A_n$ given by Eq. (8.36), is equivalent to the much simpler closed form solution of Eq. (8.25). Extraction of coefficient A_n gives

$$A_n[k_n^2 - k^2 - 2jk/z'_t L] = \frac{2jk}{L}\left[\frac{1}{z'_t}\sum_{q\neq n} (-1)^{n+q} A_q - \rho_0 c\tilde{U}\right] \quad (8.37)$$

Each coefficient A_n is seen to be a function of all other coefficients $A_{q\neq n}$. This implies that the rigid-wall modes are all mutually coupled. This is because the pressure response component expressed by each rigid-wall mode $A_n \cos(n\pi x/L)$ is partly determined by the termination particle velocity, which is itself determined by the *sum* of all the pressure terms in Eq. (8.35b). In the general case of arbitrary termination impedance, Eq. (8.37) may be solved approximately by an iterative technique (initially assuming zero coupling), or more rigorously by a variational approach; but these procedures are beyond the scope of this book.

In cases where either the real or imaginary (or both) parts of the termination impedance ratio is extremely large, as with almost impermeable structures having large mass or stiffness, the influence of the coupling term on each coefficient becomes very small, especially at frequencies close to the eigenfrequency of the rigid-wall mode concerned ($k \approx k_n$), *provided that the eigenfrequencies are well separated.* The coupling effect is further weakened by the fact that $(-1)^{n+q}$ takes alternate positive and negative values in the summation over q.

Therefore, as a first-order approximation, we may consider Eq. (8.37) with the coupling term neglected at frequencies in the close vicinity of $\omega_n = ck_n = n\pi c/L$. The

substitution of $z'_t = r + jx$ shows that the expression has a form similar to that of the resonant response of a simple oscillator to a harmonic input (Appendix 5). The small reactive part of the boundary contribution slightly alters the resonance frequency and the resistive part has the effect of a viscous damper. In the case $z'_t = r$, the equivalent viscous damping coefficient is $\zeta = c/rL\omega_n$, in agreement with Eq. (8.20b), since $\delta = \zeta\omega_n$. Consequently, under the conditions appropriate to this approximation, we may conclude that near each rigid-wall eigenfrequency, the fluid behaves predominantly like a simple, viscously damped oscillator. This model will be found to be useful when we consider the acoustical behaviour of nearly rigid-walled, reverberant rooms in the following chapter. Note that it is not valid to neglect the coupling term at frequencies remote from each rigid-wall eigenfrequency where no single mode predominates.

The above model and analysis conceals a subtlety that puzzles many students when they first become aware of it. We have expressed the pressure response to excitation by a *moving* piston, and the effect of a passively *moving* boundary, in terms of a sum over functions, each of which has zero normal gradient (therefore, *zero normal particle velocity*) at these boundaries. This apparent paradox is, of course, inherent in the general K–H integral equation. It must be realized that the Green's function introduced above is not the *solution* of the wave equation subject to the *actual* boundary conditions. It does not *satisfy* the actual boundary conditions; it simply expresses a relation between the actual normal pressure gradient at the boundary and the pressure generated in the fluid. This property is inherent in the reciprocal form of the Green's function.

The solution based upon superposition of rigid-wall modes is not well suited to energy flow computations. It is clear that sound energy cannot travel from source to termination via any *single* hard-wall mode, each of which has the form of a *pure standing wave* in which pressure and particle velocity are in quadrature. On the basis of this model, energy can only flow by means of 'collaboration' between the pressure associated with each rigid-wall mode and the particle velocities associated with others, because, in general, different modal pressure responses are not in quadrature. Solutions for intensity distributions based upon this form of model show that, whereas a good approximation to the magnitude of the pressure field, and to the stored energy, can often be obtained by truncating the modal series to include between ten and 100 terms, the intensity solution does not converge until a number of terms that is one or two orders greater is employed.

In this one-dimensional case, it is obviously much more sensible to use Eq. (8.25) than the series solution. However, in the more general three-dimensional case, the series solution is more useful, as we shall see in Chapter 9.

8.5 A simple case of structure–fluid interaction

Acoustic pressures generated in a fluid that is in contact with a structure influence its vibrational behaviour. In the majority of cases of mechanical systems operating in atmospheric air, the effect is small because the impedance of the structures greatly exceeds that of the air, even at structural resonance frequencies where the impedance is minimal. Exceptions include stiff, lightweight panels, such as the honeycomb sandwich structures used in aerospace vehicles, for which acoustic damping often exceeds structural damping, and all highly flexible panels that form the boundaries of air cavities, such as rectangular-section ventilation ducts, in which large reaction pressures are generated at the resonance frequencies of the cavities. Fluid loading profoundly

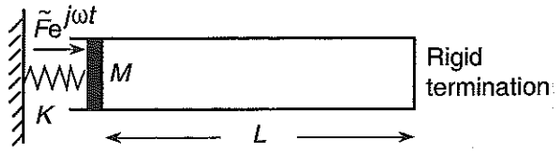

Fig. 8.8 Spring-mounted piston in a tube excited by a harmonic force.

influences the natural frequencies of structures such as marine vehicles, water tanks, and pipes that convey liquids, or gases at high pressure. This effect must be accounted for in mathematical models of such systems. For example, at low audio frequencies, the speed of bending waves in the steel hull plate structures of surface ships in contact with water is little affected by the mass of the steel and is controlled principally by the 'added' mass of the water that moves with the hull.

As a simple example of fluid–structure interaction we now consider the effect of plane waves in a fluid contained within a uniform tube on the vibrational response to a harmonic force of a sliding piston spring-mounted within the tube, shown in Fig. 8.8. The tube is assumed to be rigidly terminated. The impedances of the piston–spring system and the fluid column combine in series because they share the same particle velocity at the interface. Consequently, the mechanical impedance presented to the exciting force is that of the piston and spring in series with that of the fluid column:

$$Z_m = j(\omega M - K/\omega) - j\rho_0 c\, S \cot kL \tag{8.38}$$

in which M and K are the mass and stiffness of the piston system.

The natural frequencies of the combined system, at which the reactive component of the mechanical impedance is zero, satisfy

$$\cot kL = (M/\rho_0 SL)\, kL - (KL/\rho_0 c^2 S)/kL \tag{8.39}$$

in which $M/\rho_0 SL$ is the ratio of the masses of the piston and the fluid and $KL/\rho_0 c^2 S$ is the ratio of the stiffness of the spring to the bulk stiffness of the fluid in the tube. The solutions are indicated by the intersections of the impedance curves of the mechanical and acoustic components in Fig. 8.4(c). If the piston mass is sufficiently high and the tube sufficiently short, the fundamental natural frequency will correspond to a value of kL well below $\pi/2$, in which case the fluid reacts as a simple elastic spring. The corresponding natural frequency is given by $\omega_0^2 = \rho_0 c^2/mL$, where m is the piston mass per unit area. In this ideal system, the piston will not move at the acoustic natural frequencies of the tube blocked at both ends when $\cot kL = \infty$.

This air–spring phenomenon is of widespread importance in noise control because it operates in all air cavities at low frequencies, strongly coupling the components on either side. Among other effects, it limits the maximum vibration isolation obtainable with floating floors mounted on resilient pads, and controls the sound insulation of double-leaf walls and windows at low frequencies.

The pressure response of the fluid to a harmonic force $\tilde{F}\exp(j\omega t)$ applied to the piston is given by Eq. (8.25) with $\tilde{U}$ equal to $\tilde{F}/Z_m$ and z_t' equal to ∞. With a termination of finite impedance that has a resistive component, the response of the piston is damped by the radiation of sound energy into the tube.

8.6 Plane waves in ducts that incorporate impedance discontinuities

8.6.1 Insertion loss and transmission loss

All real duct systems incorporate geometric non-uniformities, either in the form of variations of cross-section along their lengths or locally non-uniform features such as bends, junctions and valves. Therefore, the acoustic impedance varies with position, which, in turn, implies wave reflection. Geometric non-uniformity is exploited in noise-control systems designed to attenuate sound energy transmitted along, and out of, duct systems. A common example is the expansion chamber (muffler) used to reduce the exhaust noise of internal combustion engines.

Attenuators that function on the principle of wave reflection are reactive, although many also incorporate resistive elements. In the case of a purely reactive attenuator, the principle of energy conservation demands that the rate of energy flow through the system is the same at all positions. If so, how does a reactive attenuator attenuate? The answer to this apparent paradox is that reflection reduces the *net* energy flow relative to the unattenuated case: transmitted energy equals incident energy minus reflected energy. Consequently the ongoing energy flow is reduced, just as the rate of flow of water through a garden hose is the same at every point, but you can attenuate the flow by partly closing the nozzle. (In this case the attenuation mechanism is different because the water flow rate is controlled by the balance between the static pressure loss through the system and the available supply pressure.)

Although the principle and the mechanism of reactive acoustic attenuation are clear, the matter of quantifying the effect is somewhat problematic. Two principal indices of attenuation are in common use. The 'sound power transmission coefficient' τ is defined as the ratio of transmitted power to so-called incident power. This latter term is rather misleading, since it may be confused with the *net* incident power. It is more precisely termed the 'incident-wave power'. The definition of τ also assumes that the duct section downstream of the attenuator is anechoically terminated; otherwise, it is influenced by the impedance characteristics of the whole system downstream of the attenuator. (Consider the case of the potato inserted into the end of a tail pipe.) This definition represents the performance of the attenuator *in isolation*; it is independent of any effect on upstream source power that wave reflection by the attenuator may produce by altering the load impedance presented to the source. The sound power transmission coefficient of a reactive attenuator may be expressed in terms of the acoustic impedance ratio Z' presented to an incident wave as $\tau = 4R/[(1+R)^2 + X^2]$, where $Z' = R + jX$. This is equivalent to the expression for the normal incidence sound power absorption coefficient of a plane surface (Eq. (7.23)). The logarithmic form of τ is the 'sound power transmission loss', given by $TL = 10\log_{10}(1/\tau)$ dB. It is explained diagramatically in Fig. 8.9.

A sound power reflection coefficient may be analogously defined, energy conservation demanding that the sum of the sound power transmission and reflection coefficients be unity, unless the attenuator actually generates sound, for example by producing turbulence in a flowing fluid. The sound power so generated would add to both transmitted and reflected sound power.

The 'sound power insertion loss' is defined as the logarithmic ratio of the sound power transmitted by a system before the insertion of a noise-control device to that after

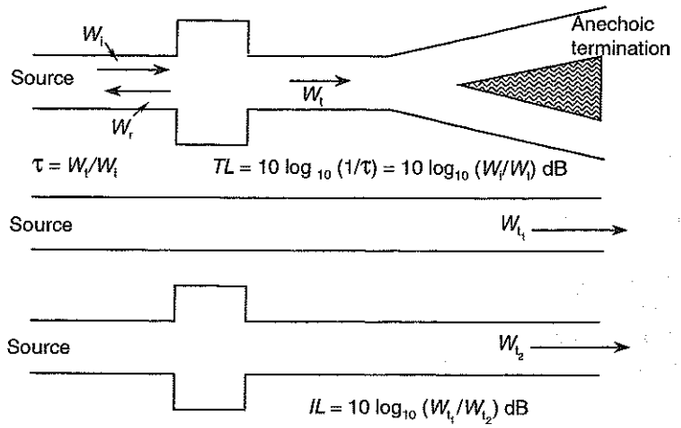

Fig. 8.9 Definitions of 'transmission loss' and 'insertion loss'.

insertion. Unlike τ, this measure not only accounts for the performance of the isolated attenuator, but also for any effects of insertion, such as alteration of source sound power, or the effects of changes to the flow regime, temperature distribution, and, most importantly, the generation of sound by the attenuator itself. Insertion loss is therefore installation sensitive, and not unique to an attenuator, but it provides a more realistic and reliable measure of attenuator performance. Insertion loss is defined in Fig. 8.9.

8.6.2 Transmission of plane waves through an abrupt change of cross-sectional area and an expansion chamber

The acoustic impedance of a uniform tube that carries only progressive plane waves is given by Eq. (4.17) as $\pm \rho_0 c/S$, where S is the cross-sectional area of the tube. If this area changes abruptly at some point, the associated change of impedance will cause incident waves to be reflected. The acoustic flow field in immediate vicinity of the area discontinuity cannot be one-dimensional and plane. Non-plane sound fields are generated but, at low frequencies, they are confined to the immediate vicinity of the discontinuity, and only plane waves can propagate and transport energy. The effect of the discontinuity is to introduce an additional inertial impedance associated with the local kinetic energy of the non-planar particle motion. It may be represented by a lumped acoustic element, as explained in Chapter 4.

In the case of a junction between two circular section tubes of considerably different diameter, as illustrated in Fig. 8.10, the inertial acoustic impedance of the junction is nearly always much less than the plane wave impedance of the narrower of the tubes, and can then be safely neglected. Consequently, plane wave pressures on either side of the junction may be assumed to be equal. As shown in Chapter 4, the elastic impedance of this local fluid region is relatively so high that it can be assumed that the volume velocities on either side of the junction are also equal.

For the purpose of studying the acoustic effect of a junction in isolation, it is assumed that it joins two anechoically terminated tubes. The harmonic wave system shown in Fig. 8.10 is represented by incident, reflected and transmitted waves of complex amplitudes $\tilde{A}$, $\tilde{B}$ and $\tilde{C}$. The junction is at $x = 0$. Pressure equality gives

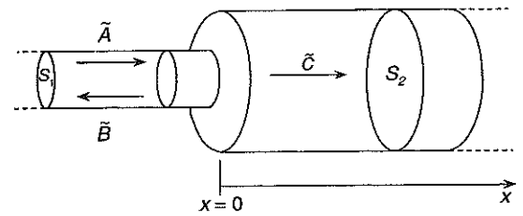

Fig. 8.10 Abrupt change in cross-sectional area.

$$\tilde{A} + \tilde{B} = \tilde{C} \tag{8.40}$$

Volume velocity equality gives

$$(S_1/\rho_0 c)(\tilde{A} - \tilde{B}) = (S_2/\rho_0 c)\tilde{C} \tag{8.41}$$

The reason why wave reflection must occur is now obvious: both equations cannot be satisfied if $S_1 \neq S_2$ and $\tilde{B}$ is zero. The solution for the ratio of transmitted to incident wave pressure amplitudes is

$$\tilde{C}/\tilde{A} = 2/(S_2/S_1 + 1) = 2m/(1 + m) \tag{8.42}$$

where $m = S_1/S_2$. Note that the pressure amplitude ratio is different for sound incident from the two directions; it is greater than unity for sound incident upon a contraction ($m > 1$) and less than unity for sound incident upon an expansion. Consequently, care must be exercised in quantifying the effect of the impedance discontinuity in terms of sound pressure levels. The reflected wave interferes with the incident wave to produce a spatial variation of pressure amplitude on the incident side of the area discontinuity. As explained above, it is safer, and less ambiguous, to define the performance in terms of the ratio of transmitted to incident sound *powers*.

The ratio of power carried by the transmitted wave to that carried by the incident wave, which is the sound power transmission coefficient of the junction, is given by the product of the cross-sectional areas and the plane wave intensities as

$$\tau = [S_2 |\tilde{C}|^2/2\rho_0 c]/[S_1 |\tilde{A}|^2/2\rho_0 c] = 4m/(1 + m)^2 \tag{8.43}$$

Unlike the pressure ratio, it is less than unity in both cases and decreases with increase in m. It is the same in both directions, or reciprocal. Since the area discontinuity is assumed to dissipate no energy, the *net* powers are equal on both sides.

The reflecting effect of a change of section is exploited in the design of internal combustion exhaust system mufflers, of which a major component is the expansion chamber, illustrated in Fig. 8.11. The acoustic impedance at the left-hand inlet (F) to the expansion chamber equals that of the larger diameter tube of length L terminated at G by that of the smaller diameter tube ($\rho_0 c/S_1$). The specific acoustic impedance transfer expression (8.24) may be adapted for acoustic impedance by replacing z'_t by the acoustic impedance ratio $z'_t = Z_t S_0/\rho_0 c$, where S_0 is the cross-sectional area of the tube to which the transfer expression applies. Hence, $Z'_G = (\rho_0 c/S_1)(S_2/\rho_0 c)$ and

$$Z'_F = Z_F S_2/\rho_0 c = (1 + jm \tan kL)/(m + j \tan kL) \tag{8.44}$$

The acoustic impedance ratio presented to the incident wave in the smaller-diameter

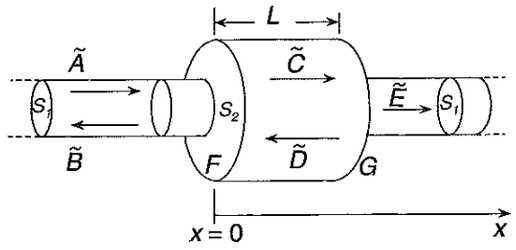

Fig. 8.11 Expansion chamber.

tube is $Z_F S_1/\rho_0 c = mZ'_F$. Now, $\tilde{B}/\tilde{A} = (mZ'_F - 1)/(mZ'_F + 1)$, giving the ratio of transmitted to incident sound powers as

$$\tau = 1 - |\tilde{B}/\tilde{A}|^2 = 4/[4\cos^2 kL + (m + m^{-1})^2 \sin^2 kL] \tag{8.45a}$$

Values derived from Eq. 8.45a for an area ratio of ten are plotted in Fig. 8.12 in terms of the sound power transmission loss. Frequencies for which $\sin kL = 0$ are the natural frequencies of the closed expansion chamber at which the impedance at F equals that at G, so that the expansion chamber is 'short circuited' and the transmission loss is zero. At intermediate frequencies corresponding to $\cos kL = 0$, the impedance ratio at F equals the *inverse* of that at G and τ takes a minimum value given by

$$\tau_{\min} = 4/(m + m^{-1})^2 \tag{8.45b}$$

The expressions derived above apply to an abrupt change of section that joins ducts of any uniform cross-section. In cases where the transition is less abrupt, such as a short conical adaptor for example, these expressions only apply approximately if the transition length is much less than a wavelength; otherwise, an acoustic horn model is required (see Section 8.11).

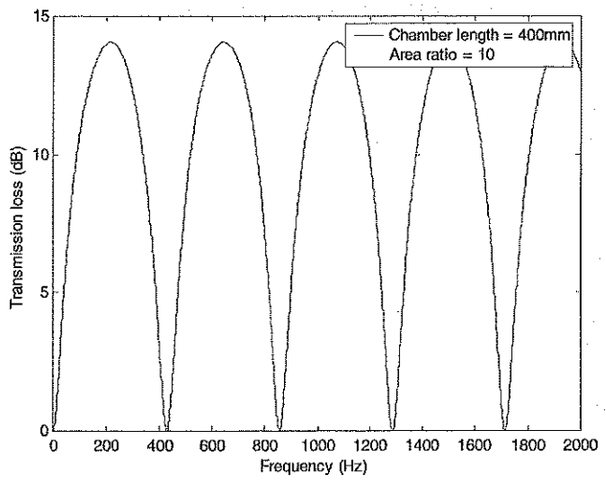

Fig. 8.12 Transmission loss produced by an expansion chamber with an area ratio of ten.

8.6.3 Series networks of acoustic transmission lines

The impedance transfer expression may be used to derive expressions for, or perform numerical studies of, the impedance of a number of transmission lines connected in series. One works away from the ultimate termination to the location of interest using a repeated application of the transfer expression, together with the insertion of lumped elements as appropriate. A disadvantage of this procedure is that the transfer expression is not a linear relation between impedances.

As an alternative, the transfer process may be formulated in terms of a 'two-port' model, which is a 'black box' relating pressure and volume velocity at the input port to the corresponding quantities at the output port. If the system is linear, the relations are linear. The pressure and volume velocity at one station of a duct system carrying only plane waves are uniquely related to the corresponding quantities at another station by the transfer properties of the intermediate system. Here we derive the transfer relations for a section of uniform duct by using the expressions for pressure and volume velocity of two oppositely travelling harmonic plane waves of different complex amplitude at two stations, one at $x = 0$ and one at $x = L$.

$$\tilde{p}(0) = \tilde{A} + \tilde{B} \tag{8.46a}$$

$$\tilde{Q}(0) = S(\tilde{A} - \tilde{B})/\rho_0 c \tag{8.46b}$$

$$\tilde{p}(L) = \tilde{A}\exp(-jkL) + \tilde{B}\exp(jkL) \tag{8.46c}$$

$$\tilde{Q}(L) = [\tilde{A}\exp(-jkL) - \tilde{B}\exp(jkL)]\, S/\rho_0 c \tag{8.46d}$$

Elimination of $\tilde{A}$ and $\tilde{B}$ transforms these equations into the two-port form as

$$\tilde{p}(0) = \tilde{p}(L)\cos kL + j\tilde{Q}(L)\,(\rho_0 c/S)\sin kL \tag{8.47}$$

$$\tilde{Q}(0) = j\tilde{p}(L)(S/\rho_0 c)\sin kL + \tilde{Q}(L)\cos kL \tag{8.48}$$

In matrix form, these become

$$\begin{bmatrix} \tilde{p}(0) \\ \tilde{Q}(0) \end{bmatrix} = \begin{bmatrix} T \end{bmatrix} \begin{bmatrix} \tilde{p}(L) \\ \tilde{Q}(L) \end{bmatrix} \tag{8.49a}$$

where

$$[T] = \begin{bmatrix} \cos kL & j(\rho_0 c/S)\sin kL \\ j(S/\rho_0 c)\sin kL & \cos kL \end{bmatrix} \tag{8.49b}$$

(Students should determine the inverse form of T and then check the product of the two.)

The principle of the two-port has already been implicitly applied in the general treatment of acoustic lumped elements in Section 4.4.1, in which two different models are presented. In one, pressure is assumed to be uniform across the element (the same at both ports) and volume velocity is different at the two ports and vice versa in the other. Consequently, acoustic lumped elements may readily be incorporated into a chain of ducts. The two-port matrix for a chain of elements is simply obtained by multiplication of the matrices that characterize individual elements. This procedure is physically more explicit than the transfer impedance approach.

For example, consider two sections of uniform duct with cross-sectional area S_1 and length L_1 connected by a length of duct of cross-sectional area S_2 and length L_2, which is

much less than a wavelength. The matrix relating the pressures and volume velocities at the inlet and outlet of the system is given by

$$\begin{bmatrix} \tilde{p}_{in} \\ \tilde{Q}_{in} \end{bmatrix} = \begin{bmatrix} T_1 \end{bmatrix}\begin{bmatrix} T_2 \end{bmatrix}\begin{bmatrix} T_3 \end{bmatrix}\begin{bmatrix} \tilde{p}_{out} \\ \tilde{Q}_{out} \end{bmatrix} \tag{8.50}$$

where the matrices $[T_1]$ and $[T_3]$ are given by Eq. (8.49b) and the matrix $[T_2]$ is obtained from Eq. (4.16) as

$$[T_2] = \begin{bmatrix} 1 & j(\rho_0 c/S_2)kL_2 \\ j\omega S_2 L_2/\rho_0 c^2 & 1 \end{bmatrix} \tag{8.51}$$

which corresponds to the matrix $[T]$ with $kL_2 \ll 1$.

With the assumption that the outlet duct is anechoically terminated, the matrix relating input to output quantities in terms of wave amplitudes may be used to obtain an expression for the sound power transmission coefficient.

8.6.4 Side branch connections to uniform acoustic waveguides

Industrial and domestic pipework systems commonly incorporate multiple branches, often connected by T-junctions as illustrated in Fig. 8.13. Sound waves travelling in any one branch will induce sound waves in all connected branches. The acoustic energy transported by the wave incident upon a branch must be conserved, unless some dissipative or generation mechanism operates within the junction. The distribution of the energy among the connected branches depends upon the relative impedances of the junctions, just as it does in an electrical circuit.

Side branch elements, such as closed-end tubes, may be attached to pipes and other forms of duct as (predominantly reactive) noise-control devices. As with the expansion chamber, the principle employed is to introduce as large as possible an impedance discontinuity in order to maximize energy reflection. It is not generally feasible to increase the junction impedance without adversely affecting the function of the pipe in transporting fluid with minimum energy loss. Consequently, one attempts to minimize the junction impedance by employing side branch resonance.

We shall assume that the frequency is sufficiently low to restrict propagation in all the connected ducts to plane waves. Hence the dimensions of the junction volume are all small compared with a wavelength. As in all cases of abrupt changes of geometry, non-planar wave motion must occur in the proximity of junctions, which implies that some non-propagating kinetic energy is locally generated. The influence of the associated

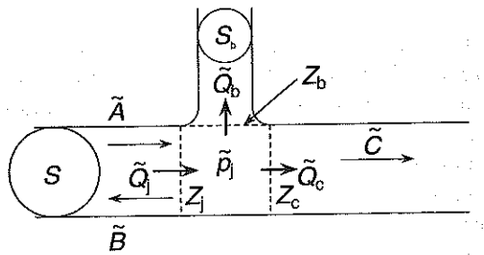

Fig. 8.13 Tee junction.

inertial impedance on the behaviour of the system depends upon its magnitude relative to the magnitudes of the impedances of the connected tubes. For the sake of simplicity, the influence is assumed to be negligible, which implies that the pressure may be assumed to be uniform over fluid in the small junction volume. Because of the very high stiffness of fluid in this volume, continuity of volume velocity through the junction may also be assumed. We denote the acoustic impedances of the junction, the branch and the continuation of the main duct beyond the branch by Z_j, Z_b and Z_c, respectively. We can now write the conditions of continuity of pressure and volume velocity in terms of complex amplitude as

$$\tilde{p}_j = \tilde{A} + \tilde{B} = \tilde{Q}_b Z_b = \tilde{Q}_c Z_c \tag{8.52a,b,c}$$

and

$$\tilde{Q}_j = (\tilde{A} - \tilde{B})S/\rho_0 c = \tilde{Q}_b + \tilde{Q}_c = \tilde{p}_j/Z_j \tag{8.53a,b}$$

Substituting $\tilde{Q}_b = \tilde{p}_j/Z_b$ and $\tilde{Q}_c = \tilde{p}_j/Z_c$ in Eq. (8.53b) gives the impedance of the junction presented to the incident wave as

$$\frac{1}{Z_j} = \frac{1}{Z_c} + \frac{1}{Z_b} \tag{8.54a}$$

or

$$Z_j = Z_b Z_c/(Z_b + Z_c) \tag{8.54b}$$

which confirms that the side branch and continuation duct are in parallel because they share the same pressure. The sound power reflection coefficient is

$$\alpha_r = |\tilde{B}/\tilde{A}|^2 = |(Z'_j - 1)/(Z'_j + 1)|^2 = \left|\frac{Z'_b Z'_c - (Z'_b + Z'_c)}{Z'_b Z'_c + (Z'_b + Z'_c)}\right|^2 \tag{8.55}$$

where $Z'_j = Z_j S/\rho_0 c$, $Z'_b = Z_b S/\rho_0 c$, $Z'_c = Z_c S/\rho_0 c$ and S is the cross-sectional area of the main duct.

The sound power transmission coefficients into the continuation duct and into the side branch are determined by expressing the transmitted powers as $\frac{1}{2}|\tilde{p}_j|^2 \operatorname{Re}\{1/Z_c^*\}$ and $\frac{1}{2}|\tilde{p}_j|^2 \operatorname{Re}\{1/Z_b^*\}$, respectively. The relation between $\tilde{B}/\tilde{A}$ and Z_j is then used to relate the power to the power transported by the incident wave. The results are

$$\tau_c = 4\left|\frac{Z'_b Z'_c}{Z'_b Z'_c + Z'_b + Z'_c}\right|^2 \operatorname{Re}\{1/Z_c'^*\} \tag{8.56}$$

and

$$\tau_b = 4\left|\frac{Z'_b Z'_c}{Z'_b Z'_c + Z'_b + Z'_c}\right|^2 \operatorname{Re}\{1/Z_b'^*\} \tag{8.57}$$

Clearly, the effect of the side branch on τ_c depends upon Z_c as well as Z_b, and therefore on the impedance characteristics of systems downstream of the side branch.

To study the influence of side branches in isolation, we now assume an anechoic termination by putting Z'_c to unity. The expressions in Eqs (8.54–8.57) become

$$Z'_j = Z'_b/(1 + Z'_b) \tag{8.58}$$

$$\alpha_r = |1 + 2\,Z'_b|^{-2} \tag{8.59}$$

$$\tau_c = 4|Z'_b/(1 + 2\,Z'_b)|^2 \tag{8.60}$$

and

$$\tau_b = 4\,\mathrm{Re}\{Z'_b\}/|1 + 2\,Z'_b|^2 = 1 - \alpha_r - \tau_c \tag{8.61}$$

as required by energy conservation.

8.6.5 The side branch tube

The side branch is assumed to take the form of a uniform tube of cross-section S_1. A closed-end side branch has an infinite terminal impedance. Its input impedance Z_b is zero at frequencies for which its length is an odd number of *one-quarter* wavelengths. Note that these are natural frequencies of a tube having one rigid termination and one pressure release termination. Equation (8.59) indicates that all the incident power is reflected at these frequencies. This is why such a side branch is often referred to as a 'quarter wave tube'. At frequencies where the length of the side branch corresponds to an integer number of half wavelengths, the impedance Z_b equals the infinite termination impedance; the side branch is effectively closed off and has no effect. Figure 8.14 illustrates the form of frequency variation of the sound power transmission loss. Note that this system performs effectively over only very small frequency ranges. In practice, it can be used to control tonal noise. However, correct tuning to the source frequency is essential, and is sensitive to gas temperature.

It might be wondered why the maximum effect does not occur at the resonance frequencies of a piston-driven, closed-end tube that correspond to the natural frequencies of a tube closed at both ends. The reason is that, unlike the piston, which is inexorably driven to produce a given *volume velocity*, the side branch is driven by the incident sound *pressure*. The impedance of the primary tube is finite, and the volume velocity driven into the side branch is maximal when the side branch impedance is minimal. This example indicates that care must be exercised when appealing to the

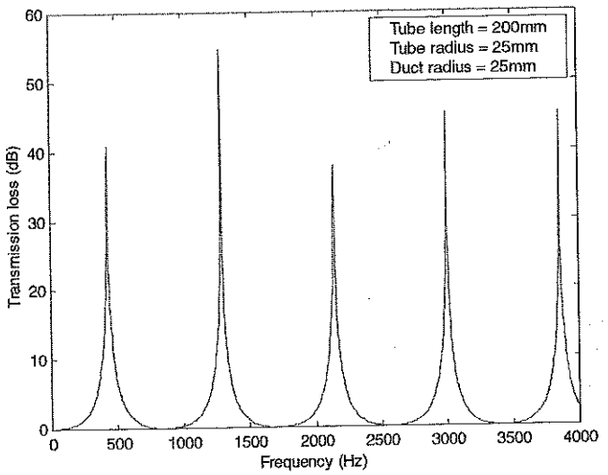

Fig. 8.14 Transmission loss produced by a closed end side tube.

phenomenon of resonance to explain acoustic phenomena in enclosed volumes of fluid; the internal impedance of the source has a crucial influence on system response and power input.

As might be expected, a tube terminated by an open end produces maximum effect at the natural frequencies close to those of a tube closed at both ends, because the inlet impedance then equals the acoustic radiation impedance of the open end, which we know to be very small at low ka. As shown in Chapter 4, the reactive component of the radiation impedance of a tube of radius a opening to free field corresponds to an additional effective length (end correction) of $0.6a$. This must certainly be applied at the free end of the side branch, but just what correction should be applied at the junction end is a moot point: it depends upon the area of the side branch relative to that of the primary tube. Readers are left to draw their own conclusions from experimental observations.

At frequencies where the side branch length corresponds to odd integer multiples of one-quarter wavelength, the entry impedance ratio is the inverse of the terminal impedance ratio, and therefore large. The side branch is effectively blocked off and has little effect. Theoretical results based upon only one end correction are presented in Fig. 8.15. In the frequency range below the lowest resonance frequency, an open-ended side branch acts as a high-pass filter from zero up to the frequency at which its length corresponds to one quarter of a wavelength, the side branch impedance corresponding approximately to that of the total mass of the fluid in the tube. It will be noticed that the maximum attenuation decreases and the bandwidth increases with frequency, reflecting the dependence of the radiation resistance on the square of frequency. Open-ended side branches are not of great interest in practice because they leak fluid as well as sound energy, although they will act in much the way indicated in Fig. 8.15 if they open into a large, fairly absorbent, closed volume.

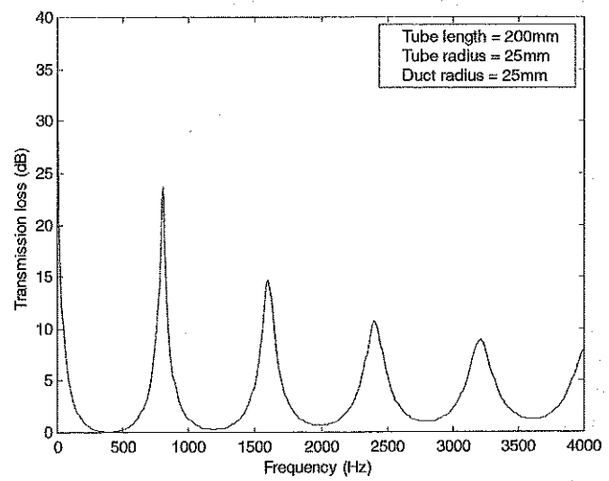

Fig. 8.15 Transmission loss produced by an open end side tube.

8.6.6 The side branch orifice

A circular aperture of radius r in the wall of a tube of radius a has an acoustic impedance ratio given approximately by $Z'_b \approx [(ka)^2/4 + j0.5(ka)(a/r)]$ when $kr \ll 1$, of which the resistive part corresponds to that of a point monopole. Unless $r/a \ll 1$, the sound pressure is very small in the vicinity of the orifice, the reflected wave being almost in antiphase with the incident wave. Equation (8.60) gives the sound power transmission coefficient as

$$\tau_c \approx (ka)^2(a/r)^2/[1 + (ka)^2\,(a/r)^2], \qquad ka \ll 1 \tag{8.62}$$

which tends to unity as r/a tends to zero. The orifice acts as a high-pass filter with a -3 dB point at a frequency given by $ka = r/a$ or $f = rc/2\pi a^2$ (for example, $r = 3$ mm, $a = 20$ mm, $f = 406$ Hz).

Although the orifice has the same practical disadvantages as an open tube, it plays a crucial role in the operation of many musical wind instruments in which the position of the first open finger/key hole controls the effective acoustic length of the air column and hence determines the pitch of the note played. One important engineering example of the exploitation of the reflective capacity of an orifice is in the diagnosis of leaks in heat exchanger tube. Short pulses of high-frequency sound are fed down the tube run and the inverted polarity and delay of the returning pressure pulse indicates the presence, size and location of any leak. Blockages are indicated by returns that are not inverted.

8.6.7 The Helmholtz resonator side branch

Side branch Helmholtz resonators may be used as reactive noise-control devices for ducts. Their low impedance in the vicinity of resonance causes strong wave reflection. The impedance ratio presented to a tube of radius a by the mouth of an undamped Helmholtz resonator, based upon expressions derived in Section 4.4.1, is

$$Z' = (\pi a^2/\rho_0 c)[R_{\text{int}} + j(\rho_0 c^2/\omega_0 V_0)((\omega/\omega_0)^3 - (\omega/\omega_0))] \tag{8.63}$$

where ω_0 is the undamped natural frequency of the resonator. For a given resonance frequency and main duct diameter, the inertial component of the impedance may be reduced by increasing the resonator volume, thereby increasing the attenuation performance. The maximum resonant attenuation decreases as the internal resistance of the resonator is increased. This is provided mainly by viscous losses in the neck, unless it is supplemented by the insertion of resistive material. Equation (8.60) gives the sound power transmission coefficient at resonance as

$$\tau_c(\omega_0) = 4[R'_{\text{int}}/(1 + 2\,R'_{\text{int}})]^2 \tag{8.64}$$

which is proportional to $(R'_{\text{int}})^2$ if $R'_{\text{int}} \ll 1$. An example is presented in Fig. 8.16. According to the lumped element model, there is only one resonance frequency. However, any resonator exhibits higher-frequency resonances associated with acoustic modes of the cavity and neck that behave as small 'rooms' (see Chapter 9). These affect sound power transmission to varying degrees. Fluid flow passing over the opening of a resonator will stimulate its resonances and generate sound. It is therefore wise to cover the aperture with a porous sheet to suppress this undesirable effect.

The radiation resistance presented by a duct to air oscillating in the side branch resonator neck is much greater than that presented by air in a large room. Consequently,

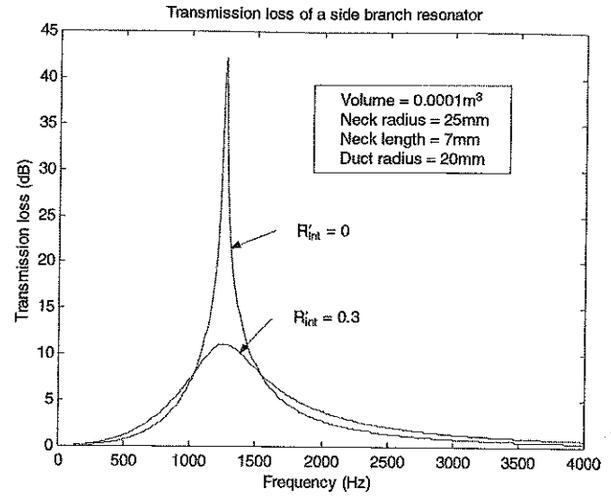

Fig. 8.16 Transmission loss produced by a side branch resonator.

a resonator has a much broader attenuation curve (effective bandwidth) in the former case.

8.6.8 Bends in otherwise straight uniform waveguides

Almost all acoustic waveguides of practical interest incorporate bends that are generally either radiused or mitred in form, although other forms such as the lobster back are also used (Fig. 8.17(a)). At frequencies at which only plane waves propagate along the straight sections, radiused bends in pipes offer little impedance change to incident waves and produce little reflection. Mitred bends present a more abrupt change in boundary geometry and generate increasingly strong reflections as the frequency approaches the lowest cut-off frequency of the waveguide (see Section 8.7.1 below). A qualitative physical explanation of this behaviour is provided by Fig. 8.17(b). The spatial phase gradient of the pressure field produced by interference between the incident plane wave and that reflected from the bend wall increases with frequency. The interference field therefore becomes increasingly less well matched to a plane wave field in the downstream leg, which has uniform phase over the cross-section. The mismatch reaches a maximum when the waveguide width equals a half wavelength. The magnitude of the reflection coefficient depends upon the specific form of duct cross-section. (Rigorous analyses can be found in references [8.1] and [8.2].)

8.7 Transverse modes of uniform acoustic waveguides

8.7.1 The uniform two-dimensional waveguide with rigid walls

So far we have assumed that our waveguides allow only axially directed plane waves to propagate. The following analysis of the sound field in a uniform, two-dimensional, infinitely extended waveguide with rigid walls serves to introduce the phenomenon of

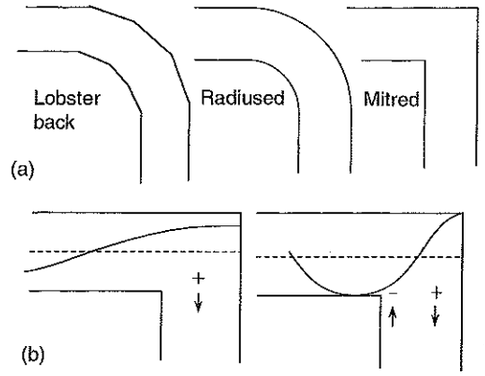

Fig. 8.17 (a) Bend geometries. (b) Qualitative explanation of transmission loss peak near to the frequency at which the wavelength equals twice the duct width.

other (higher-order) modes of propagation which are formed by interference between plane waves propagating in non-axial directions. Before embarking upon a rigorous mathematical analysis, it is worth exploring a simplified geometric model of the problem. We must first take careful note that, however complex the interference field resulting from multiple reflection of sound from the parallel walls, the acoustical disturbances that combine to form the field travel at the speed of sound. This would appear to be obvious at this point, but the results of the forthcoming mathematical analysis will give pause for thought about this fact.

Consider a *periodic* train of plane pressure pulse waves as shown by the heavy lines in Fig. 8.18(a): the exact spatio-temporal form of the pulses is immaterial to what follows. If portions of these pulse trains are to be contained within the boundaries of a uniform waveguide with rigid walls it is necessary to superimpose another train of periodic pulses (indicated by the lighter lines) in order to satisfy the boundary conditions of zero normal particle velocity *at all times*. Clearly, these correspond to the multiple reflections of the plane waves from the waveguide walls. The spatial separation (along the propagation direction) of pulses in a periodic train that propagates at any particular angle θ to the waveguide axis cannot exceed that shown in Fig. 8.18(b): but the separation can be reduced by *submultiples*, and remain periodic, as illustrated by Fig. 8.18(a). Any other positioning of a second set of periodically separated waves does not change the spatial period of the sequence. The *lowest* frequency (Hz) component of the periodic spectrum derived from a microphone placed in the waveguide is given by the speed of sound divided by the pulse spacing (that is $c/2d \sin\theta$) where d is the waveguide width and θ is the angle of the propagation direction to the waveguide axis (except on the axis where the lowest frequency has twice this value). As θ approaches $\pi/2$, this frequency approaches $c/2d$, at which the wavelength equals $2d$. This frequency is termed the 'lowest cut-off' frequency of the waveguide. The introduction of submultiple separation, as illustrated by Fig. 8.18(a), leads to the conclusion that their exists an infinite set of cut-off frequencies given by $f_n = nc/2d$, n integer.

In summary, in a duct of given width, a *particular angle* of plane pulse propagation is uniquely associated with a *harmonic series of frequencies* (for a given speed of sound in the fluid). The corollary of this statement is that any temporally harmonic sound field

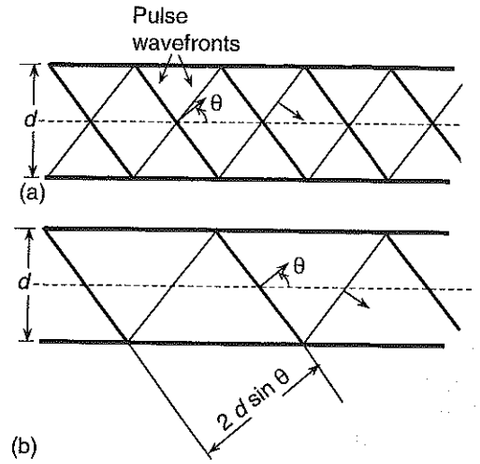

Fig. 8.18 (a) Periodically spaced plane pulses in a uniform duct with rigid walls. (b) Maximum periodic pulse spacing for a given direction of propagation.

within a waveguide may be decomposed into a set of harmonic plane waves travelling in a number of *discrete* directions, this number increasing with frequency. The plane wave directions appear in pairs, with angles $\pm\theta$. At any frequency, each pair of component plane waves produces an interference field that takes the form of a pure standing wave across the width of the duct, as shown in Fig. 8.19. Each interference *pattern* is convected along the waveguide by its parent plane waves at a speed $c/\cos\theta$, which is *greater than the speed of sound*. The total propagating field at any frequency comprises the superposition of these convected interference patterns, each pattern travelling at a different speed along the waveguide. These interference patterns are known as the 'modes' of the waveguide and the minimum propagation frequencies are known as the modal 'cut-off' frequencies of the waveguide. The plane wave is known as the 'zero-order' mode, which propagates at all frequencies and does, of course, travel along the waveguide at the speed of sound.

Having considered the geometric aspects of sound propagation in a two-dimensional waveguide, and the origin of waveguide modes in terms of component plane waves, we

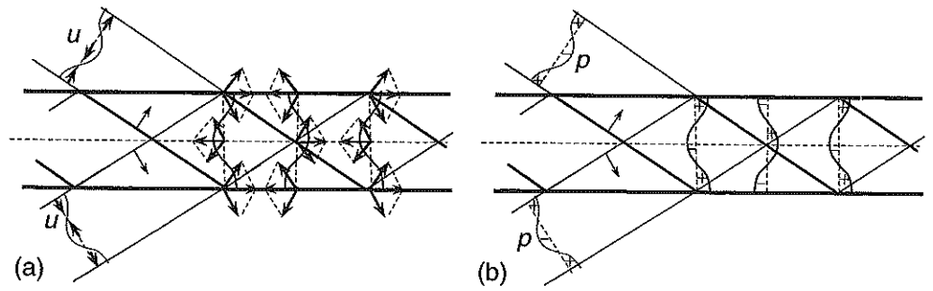

Fig. 8.19 Interference (transverse standing wave field) produced by the intersection of harmonic plane waves: (a) particle velocity; (b) pressure.

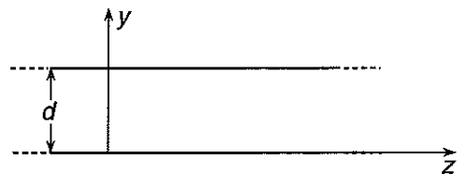

Fig. 8.20 Coordinate system for two-dimensional uniform duct.

now tackle the same problem in terms of the solution of the harmonic form of the wave equation, subject to the boundary conditions of zero normal particle velocity at the walls and infinite axial extension of the waveguide. Since energy can propagate to infinity, a harmonic field can only be sustained by a harmonic source. We initially exclude the source region from the model. The coordinate system is shown in Fig. 8.20: convention dictates that the axial coordinate is z. The acoustic pressure satisfies the two-dimensional, homogeneous Helmholtz equation, subject to the prescribed boundary conditions, as

$$\partial^2 p/\partial y^2 + \partial^2 p/\partial z^2 + k^2 p = 0 \tag{8.65}$$

together with the boundary conditions

$$\partial p/\partial y = 0 \qquad \text{at} \qquad y = 0 \text{ and } y = d \tag{8.66}$$

A trial separable expression for the spatial distribution in the form $\tilde{p}(y, z) = \tilde{A}\exp(\lambda_1 z)\exp(\lambda_2 y)$ yields

$$(\lambda_1^2 + \lambda_2^2 + k^2)\, p = 0 \tag{8.67}$$

from which the non-trivial solutions for λ_2 are

$$\lambda_2 = \pm j(\lambda_1^2 + k^2)^{1/2} = \pm j\beta \tag{8.68}$$

giving the pressure field as

$$p(z, y, t) = \exp(\lambda_1 z)[\tilde{A}\exp(-j\beta y) + \tilde{B}\exp(j\beta y)]\exp(j\omega t) \tag{8.69}$$

The boundary conditions require that

$$j\beta\exp(\lambda_1 z)[-\tilde{A}\exp(-j\beta y) + \tilde{B}\exp(j\beta y)] = 0 \tag{8.70}$$

for all values of z at $y = 0$ and $y = d$. The first condition yields

$$\tilde{B} = \tilde{A} \tag{8.71}$$

which reduces the expression in Eq. (8.69) to

$$p(z, t) = 2\exp(\lambda_1 z)\tilde{A}\cos(\beta y)\exp(j\omega t) \tag{8.72}$$

Application of the second boundary condition requires that

$$\sin \beta d = 0 \tag{8.73}$$

or

$$\beta = \pm n\pi/d, \qquad n = 0, 1, 2, \ldots \tag{8.74}$$

Substitution in Eq. (8.68) yields solutions for λ_1 and λ_2 as

$$\lambda_1 = \pm j[k^2 - (n\pi/d)^2]^{1/2}; \qquad \lambda_2 = \pm jn\pi/d \tag{8.75a}$$

with equivalent wavenumbers given by

$$k_{nz} = [k^2 - (n\pi/d)^2]^{1/2}; \qquad k_{ny} = n\pi/d \tag{8.75b}$$

The expression for the pressure field becomes

$$p_n(z, y, t) = \tilde{A}_n \exp(\pm jk_{nz}z)\cos(n\pi y/d)\exp(j\omega t), \qquad n = 1, 2, \ldots \tag{8.76}$$

At any frequency, for any value of the integer n that satisfies the condition $k > n\pi/d$, the field that propagates in the positive-z direction may be considered to be formed by the superposition of two plane waves having wavenumber vectors with components $\pm k_{ny}$ and k_{nz} in the y and z directions, respectively. The corresponding wavenumber vector diagram is shown in Fig. 8.21. The cosinusoidal pressure distribution corresponding to each value of n is characteristic of the waveguide field and is therefore defined as a waveguide mode. The first few lowest-order modal pressure distributions are illustrated by Fig. 8.22. Note that the *transverse* particle velocity component is maximum at the nodal points of zero pressure. This may be confirmed by considering the pattern of total particle velocity on the basis of the construction presented in Fig. 8.19.

The natural frequency of a mode of order n is given by $k_{nz} = n\pi/d$, or $f_n = nc/2d$. This frequency, at which the modal wavenumber vectors are normal to the waveguide axis, is also known as the modal 'cut-off' frequency, because at lower frequencies Eq. (8.75b) indicates that the axial wavenumber k_{nz} is imaginary. (Note: it has become common practice to refer to this frequency as the modal 'cut-on' frequency.) In the present case, the modal cut-off frequencies correspond to n half wavelengths in the waveguide width d.

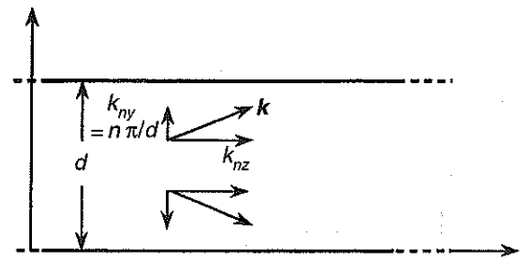

Fig. 8.21 Wavenumber vector diagram.

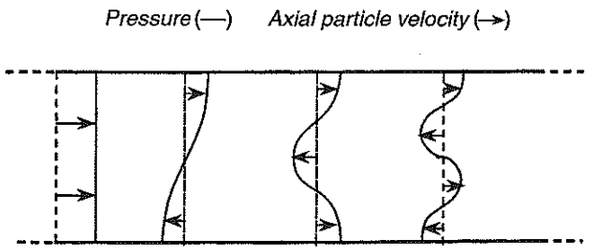

Fig. 8.22 Transverse distributions of pressure and axial particle velocity of low-order modes.

This behaviour is compatible with that inferred from the plane pulse wave construction presented above.

Above its cut-off frequency, each modal pattern of pressure (or particle velocity) propagates in the axial direction with a phase speed c_{ph} equal to ω/k_{nz}. Except for the plane wave mode, k_{nz} is always less than the acoustic wavenumber $k = \omega/c$: the corresponding phase speed is always *greater* than the speed of sound. However, readers should not be tempted to infer that acoustic disturbances, and therefore, information, can travel along the waveguide at supersonic speeds. The component plane waves that interfere to form the modal pattern each travel at the speed of sound. Consequently, it is essential to define a speed that truly represents the speed at which information (signals) can travel along the waveguide.

The speed in question is known as the 'group speed'; it corresponds in unidirectional waves to the speed of energy propagation. The group speed c_g of any wavefield in any direction is defined by $c_g = \partial\omega/\partial k$, where k is the wavenumber component in the direction concerned. In the present case, the relevant wavenumber component is k_{nz}. The group speed of a mode in the axial direction z is $(\partial k_{nz}/\partial\omega)^{-1}$, which gives

$$c_{gn} = c[1 - (n\pi/kd)^2]^{1/2} \tag{8.77}$$

which is zero at cut-off, when $k = k_{yn} = n\pi/d$, and is asymptotic to c as k tends to infinity. The variation with non-dimensional frequency kd of the phase and group speeds of a set of low-order modes is illustrated by dispersion curves in Fig. 8.23 (see Appendix 3). Multi-frequency acoustic signals are dispersed during propagation because each frequency component is distributed among the various propagating modes, each of which has a different phase velocity. The first component of the signal to arrive is that carried by the zero-order, axially propagating, plane wave. Others follow later because the component plane waves that form the higher-order modes follow a zigzag path as they repeatedly reflect from the walls.

We now turn to the question of the behaviour of a mode below its cut-off frequency. When $k < n\pi/d$, k_{nz} is imaginary and $|k_{nz}| = [(n\pi/\mathrm{d})^2 - k^2]^{1/2}$. The z-dependence of the modal field takes the form $\exp(-|k_{nz}|)z$, indicating that the modal pressure field decays

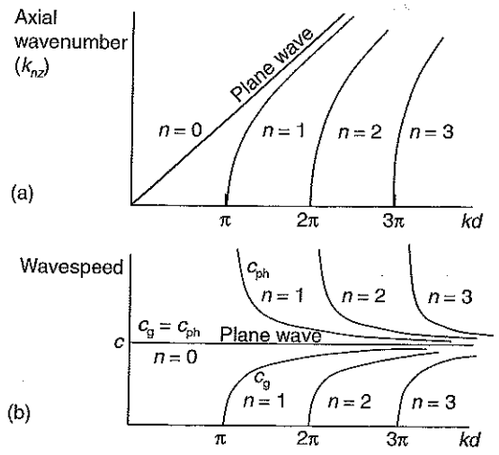

Fig. 8.23 (a) Modal dispersion curves. (b) Modal phase and group speeds.

exponentially with distance along the waveguide, the rate of decay decreasing as frequency increases towards its cut-off value. The *modal phase does not vary with z*, so the mode does not propagate as a wave and the modal pressure simply oscillates. The zero-order ($n = 0$) plane wave mode possesses no cut-off frequency and therefore propagates at all frequencies. Cut-off modes are not accounted for by the plane pulse wave construction introduced above.

8.7.2 The uniform two-dimensional waveguide with finite impedance boundaries

Sound energy travelling along a waveguide may be attenuated by lining the walls with a material layer that possesses a finite impedance having a resistive component. A reactive component will alter the spatial form and propagation speed of the sound field, but dissipates no energy. The reader is encouraged to rework the above analysis in the case of 'pressure release' boundaries. It will be found that the plane wave cannot exist because it has a uniform pressure distribution over the cross-section of a waveguide and therefore cannot satisfy the zero pressure condition. The non-zero order modal cut-off frequencies are the same as those of the rigid-walled waveguide, which means that sound cannot propagate below the lowest modal cut-off frequency. A thin plastic or rubber tube filled with water presents a good approximation to such a waveguide. This principle is used to attenuate noise propagation in liquid transport pipelines, but the flexible inner tube must be enclosed in a pressurized, gas-filled container to counteract static pressure in the liquid.

The two-dimensional waveguide model is modified by replacing the rigid walls with so-called 'impedance boundaries' that are assumed to be locally reactive. The boundary conditions of Eq. (8.66) are replaced by

$$p/(\partial p/\partial y) = jz'_w/k \tag{8.78}$$

where z'_w is the specific boundary impedance ratio. Application of the same analytical procedure as that applied to the rigid-walled waveguide yields the following transcendental equations.

For fields which are symmetric about the waveguide axis,

$$\cot[(1 + (\lambda_1/k)^2)^{1/2}(kd/2)] = -jz'_w[1 + (\lambda_1/k)^2]^{1/2} \tag{8.79a}$$

For antisymmetric fields

$$\tan[(1 + (\lambda_1/k)^2)^{1/2}(kd/2)] = -jz'_w[1 + (\lambda_1/k)^2]^{1/2} \tag{8.79b}$$

These equations must be solved numerically to obtain the modal values of λ_1 and λ_2, of which there is an infinite set of pairs. If the wall impedance has a resistive component, both λ_1 and λ_2 are complex at all frequencies, indicating that modal amplitudes decay as they propagate. This is the basis of the installation of sound-absorbent linings on duct walls to attenuate noise transmission.

Pure plane waves cannot exist in waveguides with non-rigid walls because any pressure on the wall will produce a component of particle displacement normal to the wall. Instead, the lowest-order mode is termed the 'principal mode'. Higher-order modes possess cut-off frequencies that differ from those of the rigid-wall waveguide of equal width. It is impossible to choose a wall impedance that maximizes the attenuation of all

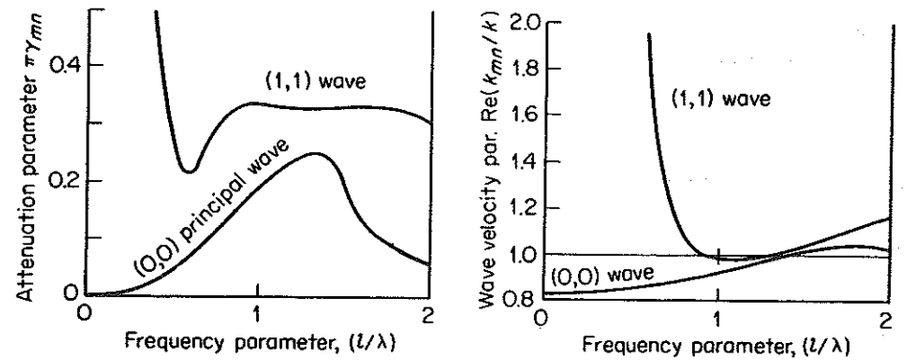

Fig. 8.24 Characteristics of the principal mode in a duct with walls of finite impedance: ℓ = duct width. Reproduced with permission from reference [8.4].

propagating modes. In practice, the principal mode usually carries the largest proportion of sound energy. For this reason, L. Cremer [8.3] proposed that the wall impedance should be selected to maximize the attenuation of this mode. The required wall impedance ratio is given by

$$z'_w = (0.930 - 0.744\,j)\,(kd/2\pi) \tag{8.80}$$

Examples of mode attenuation and phase speed are presented in Fig. 8.24, which is adapted from reference [8.4]. Further examples of calculated attenuation performance are presented in Section 8.10.

8.7.3 The uniform waveguide of rectangular cross-section with rigid walls

A simple extension of the analysis presented in Section 8.7.1 to waveguides of rectangular cross-section having dimensions a and b shows that the modal pressure takes the form

$$\tilde{p}_{mn}(x, y, z) = \tilde{A}_{mn} \exp(\pm jk_{mn}z) \cos(m\pi x/a) \cos(n\pi y/b) \tag{8.81}$$

where $k_{mn} = [k^2 - (m\pi/a)^2 - (n\pi/b)^2]^{1/2}$. The modal cut-off frequencies are given by

$$f_{mn} = (c/2\pi)\,[(m\pi/a)^2 + (n\pi/b)^2]^{1/2} \tag{8.82}$$

The cross-sectional regions of uniform phase for some low-order modes are shown in Fig. 8.25. The regions are separated by nodal surfaces of zero pressure and maximum transverse particle velocity.

8.7.4 The uniform waveguide of circular cross-section with rigid walls

The wave equation in cylindrical coordinates is used to analyse sound fields in waveguides of circular cross-section so that the wall boundary condition may be associated with a fixed value of the radial coordinate. This coordinate system is shown in Fig. 8.26. The Helmholtz form of the equation is stated without proof as

$$\frac{\partial^2 p}{\partial r^2} + \frac{1}{r}\frac{\partial p}{\partial r} + \frac{1}{r^2}\frac{\partial^2 p}{\partial \phi^2} + \frac{\partial^2 p}{\partial z^2} + k^2 p = 0 \tag{8.83}$$

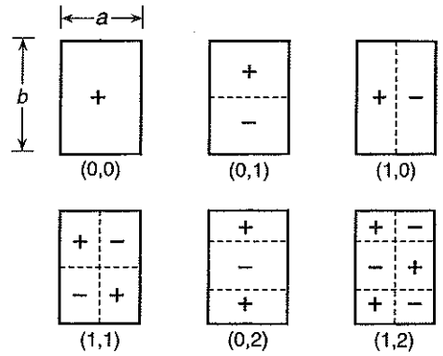

Fig. 8.25 Regions of uniform phase in low-order modes of a uniform waveguide of rectangular cross-section.

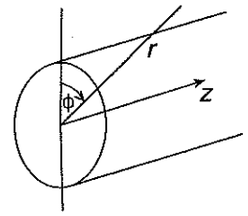

Fig. 8.26 Cylindrical coordinate system.

Modal solutions of this equation subject to a rigid wall condition at $r = a$ are

$$\tilde{p}_{mn}(r, \phi, z) = \tilde{A}_{mn} J_m(k_r r) \begin{matrix}\cos\\ \sin\end{matrix} (m\phi) \exp(-jk_z z) \tag{8.84}$$

where $J_m(k_r r)$ is the Bessel function of order m and $k_r^2 + k_z^2 = k^2$. Just as the trigonometric functions $\sin x$ and $\cos x$ are defined by series in powers of x, the Bessel function of order m is defined by the series

$$J_m(x) = \frac{\left(\frac{1}{2}x\right)^m}{m!} - \frac{\left(\frac{1}{2}x\right)^{m+2}}{1!\,(m+1)!} + \frac{\left(\frac{1}{2}x\right)^{m+4}}{2!\,(m+2)!} + \ldots \tag{8.85}$$

Bessel functions of orders one and two are shown in Fig. 8.27. The rigid wall boundary condition corresponds to the points of zero radial pressure gradient indicated on the figure. The radial particle velocity component is maximum at the points of maximum gradient. The rigid wall boundary condition constrains k_r to take an infinite set of discrete values that depend upon m and n.

The cosine product proper to the modes of a rectangular section duct is replaced by a product of cos/sin functions of the angular coordinate ϕ and a Bessel function which describes the radial variation of pressure. The cos/sin functions exhibit radial lines of zero pressure (nodal surfaces) that occur at angular intervals of π/m. The circumferential particle velocity component is maximum at these surfaces. The cross-sectional regions of

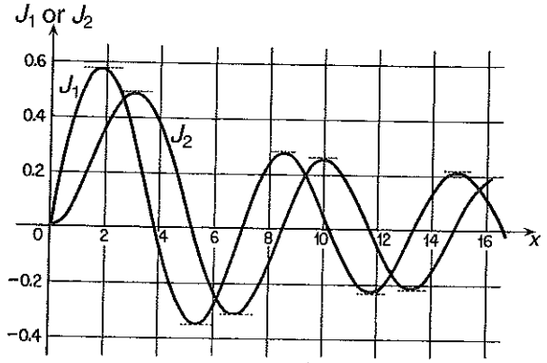

Fig. 8.27 Bessel functions with points of zero gradient indicated. Reproduced with permission from Miller, K. S. (1956) *Engineering Mathematics*. Reinhardt, New York.

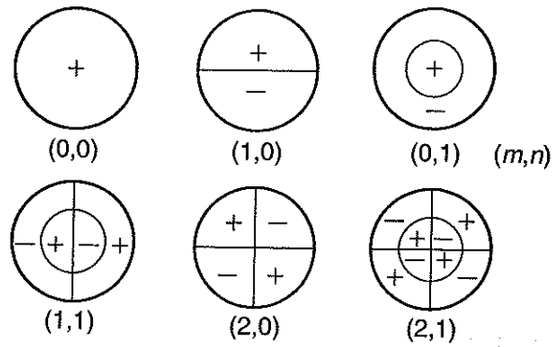

Fig. 8.28 Regions of uniform phase in low-order modes of a uniform, circular cylindrical waveguide.

uniform phase for low-order modes are shown in Fig. 8.28. Circular section waveguides exhibit the phenomenon of modal cut-off, the cut-off frequencies for a selection of low-order modes being presented in Table 8.1.

The lowest cut-off frequency is given by $ka = 1.84$, or $\lambda = 1.7$ times the diameter compared with twice the width of a square section waveguide.

8.8 Harmonic excitation of waveguide modes

The fluids in practical waveguides such as ventilation ducts and industrial pipes are excited by a great diversity of sources. Positive displacement pumps and internal combustion engine exhaust flows operate essentially as Category 1 volume/mass displacement sources. Axial fans in ducts operate principally as Category 2 force sources, generating mean pressure changes in the fluid. Flow-control valves produce turbulence that results in fluctuating forces on the solid components, the reaction forces

Table 8.1 Cut-off frequencies of acoustic modes of hard-walled ducts of circular cross-section[a]

	n				
m	0	1	2	3	4
0	0	3.83	7.02	10.17	13.32
1	1.84	5.33	8.53	11.71	14.86
2	3.05	6.71	9.97	13.17	16.35
3	4.20	8.02	11.35	14.59	17.79
4	5.32	9.28	12.68	15.96	19.20
5	6.42	10.52	13.99	17.31	20.58
6	7.50	11.73	15.27	18.64	21.93
7	8.58	12.93	16.53	19.94	23.27
8	9.65	14.12	17.77	21.23	24.59

[a] Values of $k_{rs}a\,(=ka)$ are tabulated.
Adapted from *Sound and Structural Vibration* (Fahy, 1987) – see Bibliography.

constituting Category 2 sources. They also generate sound by means of turbulent mixing, which constitutes a Category 3 source.

Clearly, in this textbook, it is impractical and inappropriate to attempt to analyse the effects of real source complexity or the effects of mean flow, viscosity, non-uniform temperature, boundary layers and turbulence on sound propagation. Consequently, the following analysis is confined to excitation by a harmonic point monopole source of an infinitely extended waveguide of rectangular cross-section containing an otherwise quiescent fluid. Any other more complex source may be synthesized in terms of a spatial distribution of monopoles.

A point monopole source generates a sound field that is symmetric about any plane in which it is located. Hence it may be considered that the plane represents an otherwise rigid boundary. We define this plane to lie at $z = 0$. The axial particle velocity normal to this plane may be represented by the delta function distribution

$$u_n(x, y, t) = \tfrac{1}{2}\tilde{Q}\,\delta(x - x_0)\,\delta(y - y_0)\exp(j\omega t) \tag{8.86}$$

where $\tilde{Q}$ is the volume strength of the monopole. The pressure field in the region $z > 0$ may be represented by an infinite sum over modes expressed by Eq. (8.81) with a negative sign in the exponent. The axial particle velocity of the field is obtained by the application of the z-directed momentum equation to allow the equality of source and field axial particle velocities on the plane to be expressed by

$$(k_{mn}/\omega\rho_0)\,\tilde{A}_{mn}\cos(m\pi x/a)\cos(n\pi y/b) = \tfrac{1}{2}\tilde{Q}\,\delta(x - x_0)\,\delta(y - y_0) \tag{8.87}$$

Multiplication of both sides of the equation by $\cos(p\pi x/a)\cos(q\pi y/b)$, followed by integration over the area of the plane, yields, by virtue of the orthogonality of the cosine functions,

$$(k_{mn}/\omega\,\rho_0)\,\tilde{A}_{mn}\,\varepsilon_{mn}\,ab = 2\tilde{Q}\cos(m\pi x_0/a)\cos(n\pi y_0/b) \tag{8.88}$$

in which $\varepsilon_{mn} = 4$ with $m = n = 0$; $\varepsilon_{mn} = 2$ with m or $n = 0$, $m \neq n$; and $\varepsilon_{mn} = 1$ with $m \neq 0$, $n \neq 0$.

The total pressure field is given by

$$p(x, y, z, t) = \exp(j\omega t)\sum_{m}^{\infty}\sum_{n}^{\infty}\tilde{A}_{mn}\cos(m\pi x/a)\cos(n\pi y/b)\exp(-jk_{mn}z) \quad (8.89)$$

with the complex pressure amplitude of mode given by

$$\tilde{A}_{mn} = \frac{2\omega\rho_0\tilde{Q}\cos(m\pi x_0/a)\cos(n\pi y_0/b)}{k_{mn}\,\varepsilon_{mn}ab} \quad (8.90)$$

in which $k_{mn} = [k^2 - (m\pi/a)^2 + (n\pi/b)^2]^{1/2}$. For the plane wave mode ($m = n = 0$), $\tilde{A}_{00} = \rho_0 c\tilde{Q}/2ab$.

Each modal amplitude is seen to be proportional to the value of the modal cross-sectional pressure distribution at the location of the source and to increase towards infinity at the modal cut-off frequency. In practice, real sources possess finite internal impedance, which limits the effect, but modal pressures do exhibit very large values close to the corresponding cut-off frequencies. The amplitudes of modal fields that are excited below their cut-off frequencies decay exponentially with distance from the source. Their presence allows the near field in the close vicinity of the monopole source, which is not affected by wave reflection, to approach that of the monopole in isolation.

The sound field generated by a point source in a hard-walled duct of rectangular cross-section may also be determined by the use of an image source model, in which wall reflections are replaced by an infinite set of source images distributed over the plane $z = 0$ as shown in Chapter 9. This model is more useful than the modal model for representing the field in the vicinity of a source plane, because the resulting summation of free-field Green's functions converges more rapidly than the modal sum. The contrary holds far from the source plane. Students are urged to write computer programs to check this.

Division of the expression in Eq. (8.89) by $-j\omega\rho_0\tilde{Q}\exp(j\omega t)$ gives the Green's function of the fluid, which satisfies the rigid boundary condition $\partial g/\partial n = 0$ at the walls in the region $z > 0$. According to the K–H equation, this function, together with its companion for the region $z < 0$, may be used to determine the response of the fluid in a waveguide to a *specified* field of wall vibration. If the walls are rather flexible, as in the case of rectangular section heating, ventilation and air-conditioning ducts, or a duct contains a liquid of high impedance, the K–H integral must be solved together with the equation of motion of the walls. This is a complicated problem of structure–fluid interaction, of which a simple example is presented in Chapter 9.

8.9 Energy flux in a waveguide of rectangular cross-section with rigid walls

The time-average intensity in any harmonic sound field is given by $\frac{1}{2}\,\mathrm{Re}\{\tilde{p}\tilde{u}^*\}$, where $\tilde{p}$ and $\tilde{u}$ are the complex amplitudes of pressure and particle velocity. The *transverse* intensity of an *isolated* mode in a hard-walled duct is zero because the transverse component of particle velocity is in quadrature with the pressure. The axial intensity distribution is given by

$$I_{nz} = (1/2\,\omega\rho_0)\,\mathrm{Re}\{k_{mn}\}\,|\tilde{A}_{mn}|^2\,[\cos(m\pi x/a)\cos(n\pi y/b)]^2 \quad (8.91)$$

The axial intensity of individual modes excited below their cut-off frequencies is zero. The modal power per unit modal pressure amplitude is zero at the cut-off frequency and asymptotic to $(\varepsilon_{mn}/4)$ times the plane wave power at very high frequency.

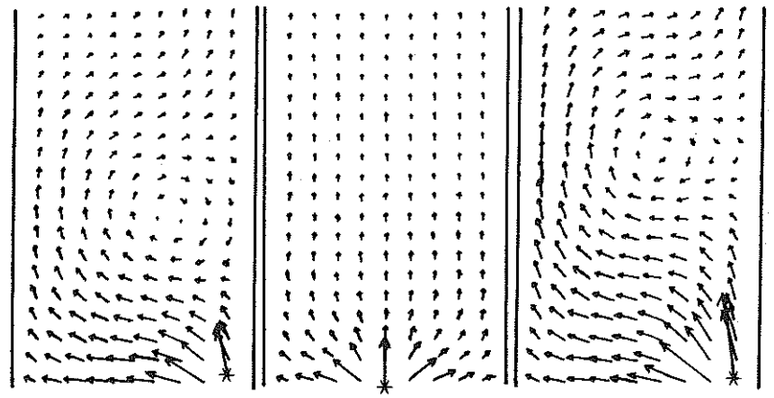

Fig. 8.29 Mean intensity distributions in a uniform, rigid-walled duct excited by a point monopole (duct width = 1 m, f_{10} = 168 Hz; vector scale $\sim I^{1/4}$). Reproduced with permission from reference [5.1].

The isolated mode picture is simplistic, because the pressure in one mode can cooperate with the particle velocity in another that is excited at the same frequency. Consequently, we must extend the intensity expressions to include all the modes. This results in an extremely complicated intensity vector field in which, close to a source, even the cut-off modes take part. As noted in Chapter 5, the time-average intensity generally exhibits circulatory patterns in interference fields, of which the waveguide field is an example. The effect is illustrated by Figs 8.29(a–c), which show the calculated intensity fields in a two-dimensional duct excited by a line monopole source (to preserve two-dimensionality). The effect of the presence of the first-order mode is clearly seen in the patterns of Fig. 8.29(a), in which it is excited just below cut-off, and Fig. 8.29(c), in which it is excited just above cut-off. When the source is centrally located, at the nodal point of this mode, its influence disappears, as seen in Fig. 8.29(b).

The complexity of the intensity pattern generally increases with frequency. However, when such an intensity field is integrated over a wide frequency band, representing excitation by a broadband source (which is valid by virtue of the independence of intensities associated with sound fields of different frequencies), the complexity largely disappears and the direct field of the source becomes evident. This feature applies not only to intensity fields, but also to spatial distributions of *mean square* pressures and particle velocities, and hence to energy density distributions. The implication for models, predictions and measurements of mean square pressure fields in enclosures is profound, as we shall see in the following chapter. It may be qualitatively explained by graphically superimposing the mean square distributions of many standing waves of different wavelength – the spatial fluctuations average out to produce a 'smoother' field.

Integration of the total axial intensity over the cross-section of the duct demonstrates that the total power transported by the duct is equal to the sum of the powers transported by each mode, as a result of modal orthogonality.

8.10 Examples of the sound attenuation characteristics of lined ducts and splitter attenuators

Extensive numerical studies of the attenuation of sound in two-dimensional, uniform ducts produced by resistive wall linings are presented in *Sound Absorption Technology* (Ingard, 1994 – see Bibliography). The resistance ratio of the wall lining is given by $R = \sigma d/\rho_0 c$, where σ is the material flow resistivity and d is the lining width. Examples of theoretical attenuation rates per air channel width are presented in Figs 8.30(a) and (b) for various values of R as a function of frequency in terms of the parameter channel

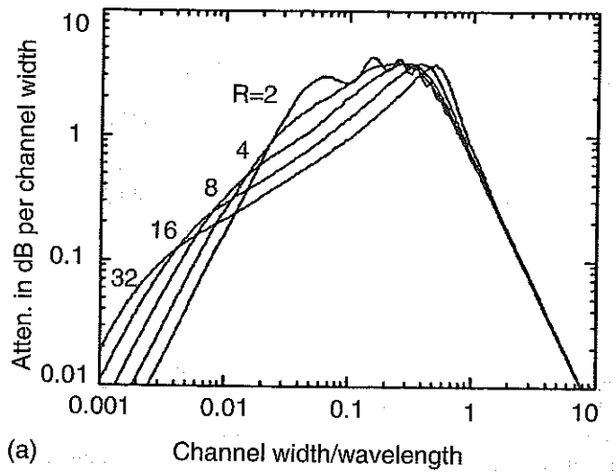

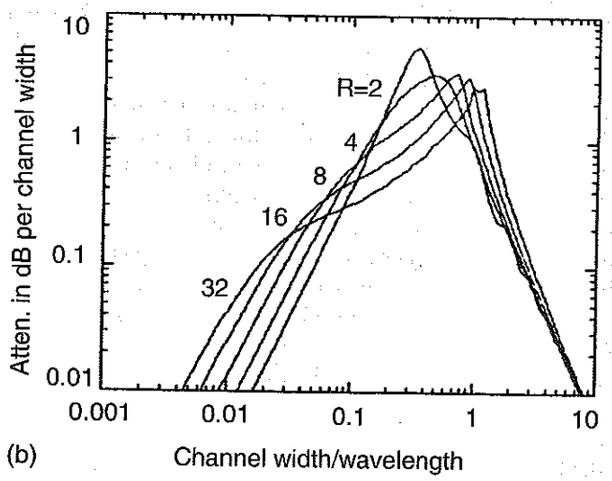

Fig. 8.30 Attenuation of the fundamental mode in a rectangular duct with one side lined with a *locally reacting* porous layer of thickness d with a total normalized flow resistance R. Channel width = D and fraction open duct area = $D/(d + D)$: (a) 20% open duct area; (b) 70% open duct area. Reproduced with permission from Ingard, K. Uno (1994) *Sound Absorption Technology*. Noise Control Foundation, Poughkeepsie, NY.

width/wavelength. It will be observed that the maximum value of about 4 dB per channel width is largely independent of R (for $R > 2$), although the low-frequency performance increases monotonically with R and the mid-frequency performance decreases monotonically with R. The effective bandwidth increases with the ratio of lining to duct width. Note that the maximum occurs in a frequency range around the first-order mode cut-off frequency of the equivalent rigid-walled duct, where the channel width equals half a wavelength. Many duct lining materials used in practice do not exhibit local reaction. The analysis of the resulting coupled waves that propagate in both the air and the lining is beyond the scope of this book.

For practical reasons to do with problems of physical robustness, acoustic resonances in linings and the attenuation of higher-order modes, it is more effective to subdivide the airway of large ventilation ducts, which may exceed 2 m in width, by means of lined splitters, as illustrated by Fig. 8.31. An example of the performance of a splitter attenuator is presented in Fig. 8.32. A set of splitters reflects some of the energy of incident waves reactively through the change of area (impedance) at entry; the opposite change at exit effects further reflection back into the attenuator. The engineering design challenge is to maximize attenuation while minimizing the mean pressure loss across an

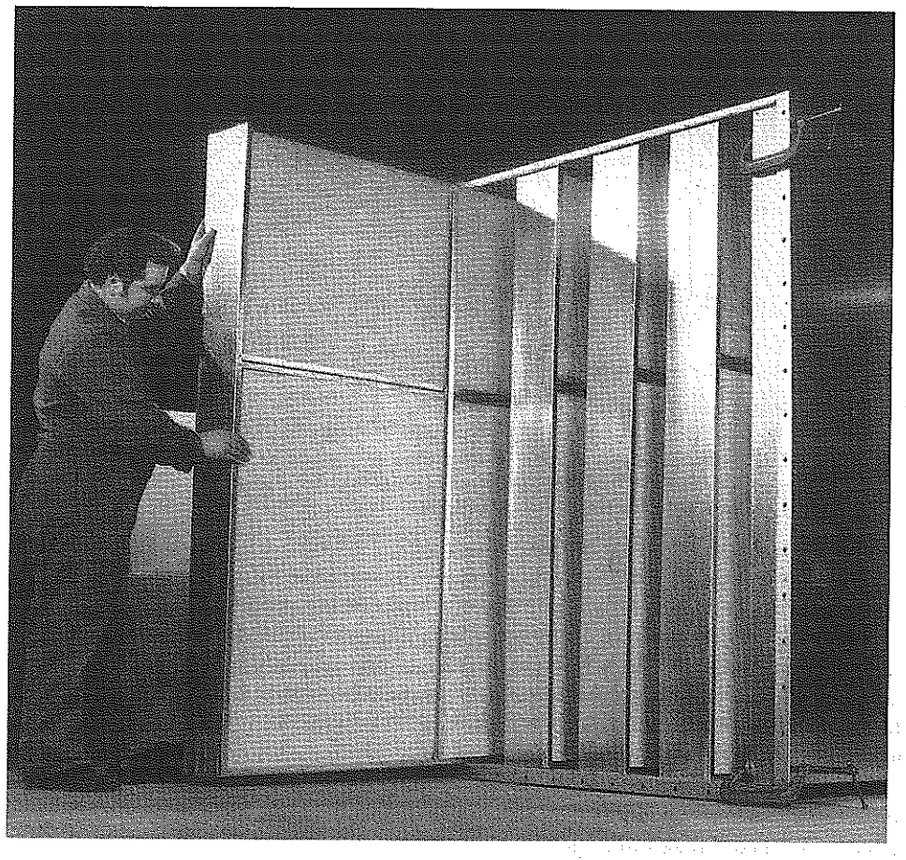

Fig. 8.31 A splitter attenuator. Courtesy of Salex Group of Companies.

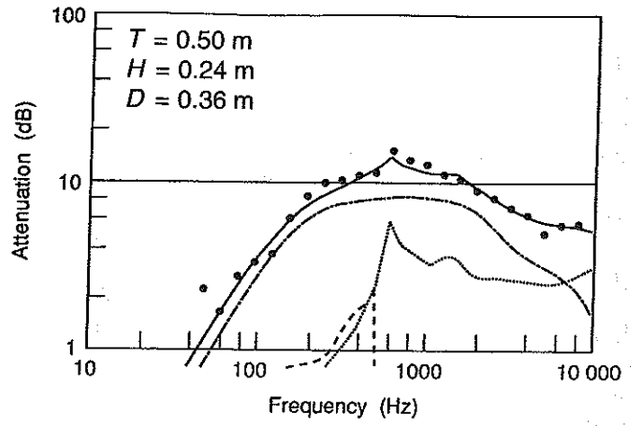

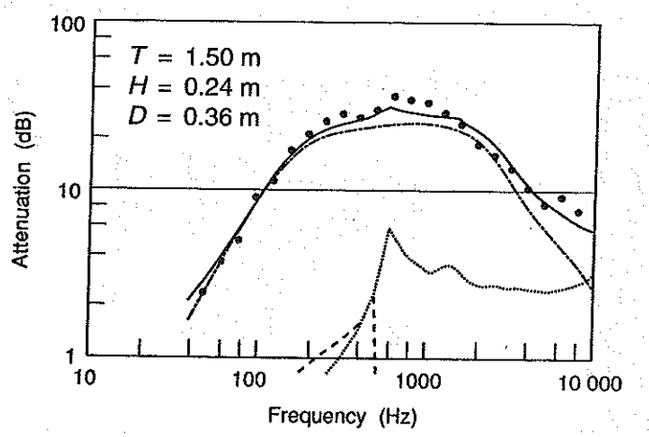

Fig. 8.32 Typical performance of a splitter attenuator showing the contributions from the liner, and the inlet and outlet reflections. T = baffle length; H = airway width; D = splitter thickness: •, experiment; ———, theory; – · – · –, theory – propagation loss; ·····, theory – entry reflection loss; – – – –, theory – exit reflection loss. Reproduced with permission from Mechel, F. P. (1990) Numerical results to the theory of baffle-type silencers. *Acustica* **72**: 7–20.

attenuator, which significantly affects the power needed to produce the required air flow. The A-weighted noise spectra of the centrifugal fans that drive most heating, ventilation and air-conditioning systems in large buildings tend to peak in the 63–125 Hz octave bands, for which attenuator performance is generally well below peak. Consequently, the length of attenuator required to meet a delivered noise specification is largely determined by the performance in these bands.

The walls of rectangular-section ducts are quite flexible. Wall vibration induced by a sound field in a duct produces two important effects: sound is radiated into the external space – so-called 'break out'; and the propagation and attenuation of acoustic modes in the duct are altered, as shown in reference [8.5].

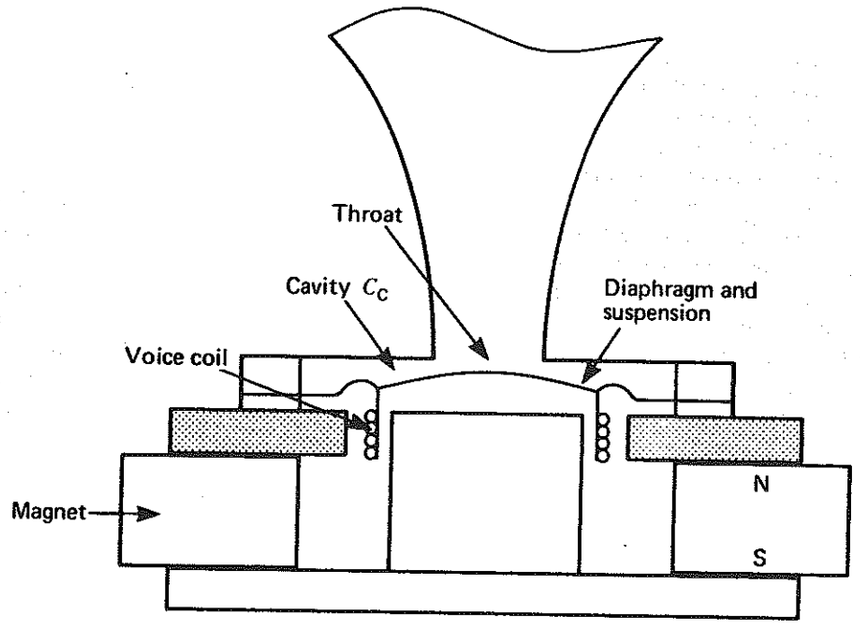

Fig. 8.33 Schematic of an audio horn and driver. Reproduced from Borwick, J. (ed.) (1988) *Loudspeaker and Headphone Handbook*. Butterworth, London.

8.11 Acoustic horns

8.11.1 Applications

Acoustic horns are best known as components of high-power, broadband audio systems in which a so-called 'compression driver' comprising a small diameter, lightweight diaphragm suspended in an enclosure is attached to the smaller end (the throat) of a horn and sound is emitted from the larger end (the mouth), as shown in Fig. 8.33. They are most commonly used in public address systems and in sound reinforcement systems in large auditoria, stadia and public spaces, which require high-level sound to be accurately directed over large distances. Especially short forms of folded horn are incorporated in megaphones.

Direct radiator loudspeakers, which are sources of volume velocity, offer fewer practical advantages, and a number of disadvantages, for such applications. Over the lower part of the operational frequency range, the cone moves more or less as a rigid body and the sound power radiated by such a source is given by the time-average product of the volume velocity and the space-average sound pressure acting on the diaphragm (cone). At any individual frequency, the time-average power is given by the product of the mean square volume velocity and the real part of the specific acoustic radiation impedance. As we know from Section 6.6, the diaphragms of direct radiator loudspeakers, which radiate like rigid pistons in the lower part of their frequency range, are very inefficient at low ka, the specific radiation resistance ratio being very much less than unity. The result is that almost all of the electrical power fed to the loudspeaker is dissipated in the driving coil, typically less than 1% being radiated as sound. Individual

direct radiators are more or less omnidirectional at low frequencies and therefore not well suited to public address, although arrays of units (columns) are rather effective in this respect. In general, direct radiators are not suitable for applications that require high sound power output over the frequency range most important for speech intelligibility (broadly 800–3500 Hz).

Clearly high power, together with acceptable reproduction quality and high electro-acoustic efficiency (acoustic power radiated/electrical power consumed), require a high volume velocity in combination with a high specific radiation resistance that is not too frequency dependent. The mass of a diaphragm tends to increase at a greater rate than its area, because of the requirement for stiffness, and the velocity produced at any frequency by a given magnetic force is inversely proportional to mass. Volume velocity equals velocity times area. Hence, there is advantage to be had in using a stiff, lightweight diaphragm of small diameter, provided that an appropriately high radiation resistance can be offered to it. The highest frequency-independent specific acoustic resistance that can be presented to a compact source of volume velocity is that offered by an anechoically terminated, uniform tube of the same cross-sectional area. If a tube is uniform and terminated by a simple opening, reflections from the open end will cause both the input resistance and reactance impedance to vary strongly with frequency, as shown earlier in this chapter. This is clearly not a recipe for faithful sound reproduction. The acoustic horn provides a solution to this problem by offering a waveguide in which a smooth transition takes place between the small throat and a large mouth. Because of its large area, the mouth allows efficient radiation of energy into the surrounding fluid, and therefore minimizes reflection back to the throat. The directivity of energy radiation is controlled by the shape of the wavefront at the mouth and also by the shape of the periphery of the horn mouth through the phenomenon of diffraction (see Chapter 12).

Acoustic horns are not only of interest to audio engineers. They feature in high-intensity test facilities for aerospace structures, in particle agglomeration systems for pollution control, as noise sources for acoustic wind tunnels, and in anechoic terminations of flow ducts, among others. The acoustical behaviour of ducts that vary in cross-sectional area along portions of their lengths are of concern to engineers because they feature commonly as adaptors in industrial ductwork. Solid horns are used 'in reverse' to concentrate the ultrasonic energy generated by large-diameter crystals into small areas for purposes such as dental drilling, machining of various forms and surface cleaning.

8.11.2 The horn equation

This section introduces a form of the wave equation, known as Webster's horn equation, which applies exactly to a small family of horn geometries that support so-called one-parameter (1-P) sound fields. It also applies approximately to a larger set of horns with uniform cross-section shapes, and cross-sectional areas that vary smoothly and monotonically along their lengths. Solutions to Webster's equation are not explicitly derived because they are more appropriately elaborated elsewhere (e.g., *Vibration and Sound* (Morse, 1948), and *Acoustical Engineering* (Oslen, 1991), listed in the Bibliography). A very thorough exposition of the subject of Webster's equation and 1-P wave fields is presented by Putland [8.6]. The impedance characteristics of a range of horns of simple geometry are presented graphically to illustrate the features that distinguish them from uniform tubes.

Figure 8.34 shows wavefronts bounding a fluid element in a diverging waveguide. The

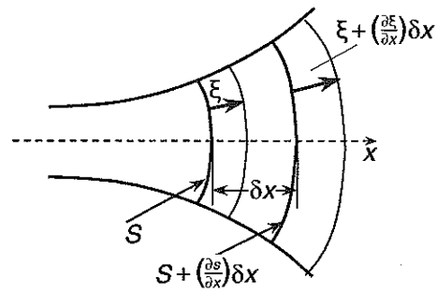

Fig. 8.34 Fluid element in a horn.

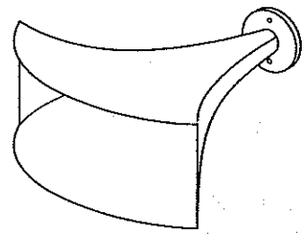

(a) An exponential horn

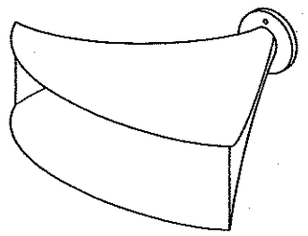

(b) A sectoral horn

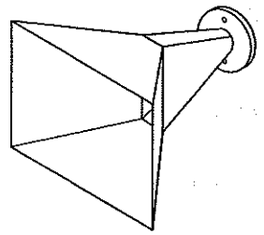

(c) A constant directivity horn

Fig. 8.35 A variety of horn shapes. Reproduced with permission from Holland, K. R. (1992) A study of the physical properties of mid-range loudspeaker horns and their relationship to perceived sound quality. PhD Thesis, University of Southampton.

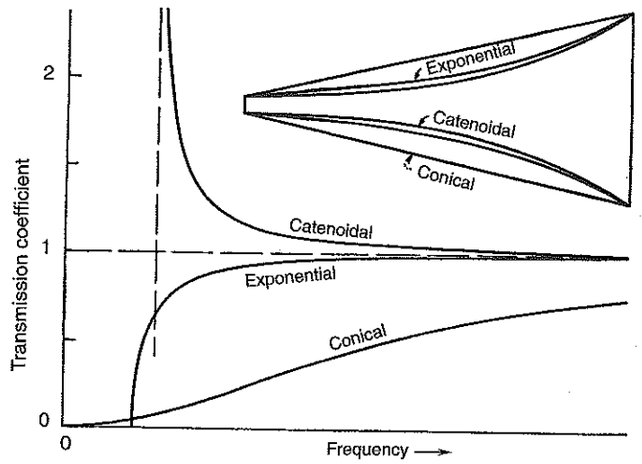

Fig. 8.36 Transmission ratios of ideal, infinite horns of analytic form. Reproduced with permission from Morse, P. M. (1948) *Vibration and Sound*, 2nd edn. McGraw-Hill, New York.

wavefronts, which have surface area $S(x)$, are assumed to be self similar and the sound pressure and particle velocities (directed normally to the wavefronts) are assumed to be uniform over the wavefronts. As required by the boundary condition on pressure gradient normal to a boundary, the wavefronts intersect the boundary at right angles. (Note: this condition is not satisfied by plane waves, which are often assumed.) All fluid elements lying between any two closely spaced wavefronts are subject to the same conditions and therefore any one may be selected as the subject of the following equations. The generalized 1-P coordinate is orthogonal to the local wavefront.

The volumetric strain is

$$\varepsilon = \{S\xi - [S + (\partial S/\partial x)\,\delta x]\,[\xi + (\partial \xi/\partial x)\,\delta x]\}/S\,\delta x \tag{8.92}$$

which, provided that $\partial S/\partial x$ is sufficiently small, ε becomes $(1/S)\,\partial(S\xi)/\partial x$ to first order.

The acoustic pressure is therefore given by

$$p = -\rho_0 c^2\,\varepsilon = -(\rho_0 c^2/S)\,\partial(S\xi)/\partial x \tag{8.93}$$

The linearized momentum equation is

$$\partial p/\partial x = -\rho_0\,\partial^2 \xi/\partial t^2 \tag{8.94}$$

Differentiation of Eq. (8.93) twice with respect to t, and of Eq. (8.94) with respect to x, yields the wave equation

$$\frac{S}{c^2}\frac{\partial^2 p}{\partial t^2} = \frac{\partial}{\partial x}\left[S\frac{\partial p}{\partial x}\right] \tag{8.95}$$

Only two geometric forms of horn allow purely 1-P progressive wave solutions analogous to the plane wave, in which the intensity varies inversely with S, so that waves progress without reflection. These are the conical horn and the cylindrical sector horn shown in Fig. 8.35. Other forms of axisymmetric horn that support 'almost' 1-P waveforms are the exponential and catenoidal horns, of which sections are shown in

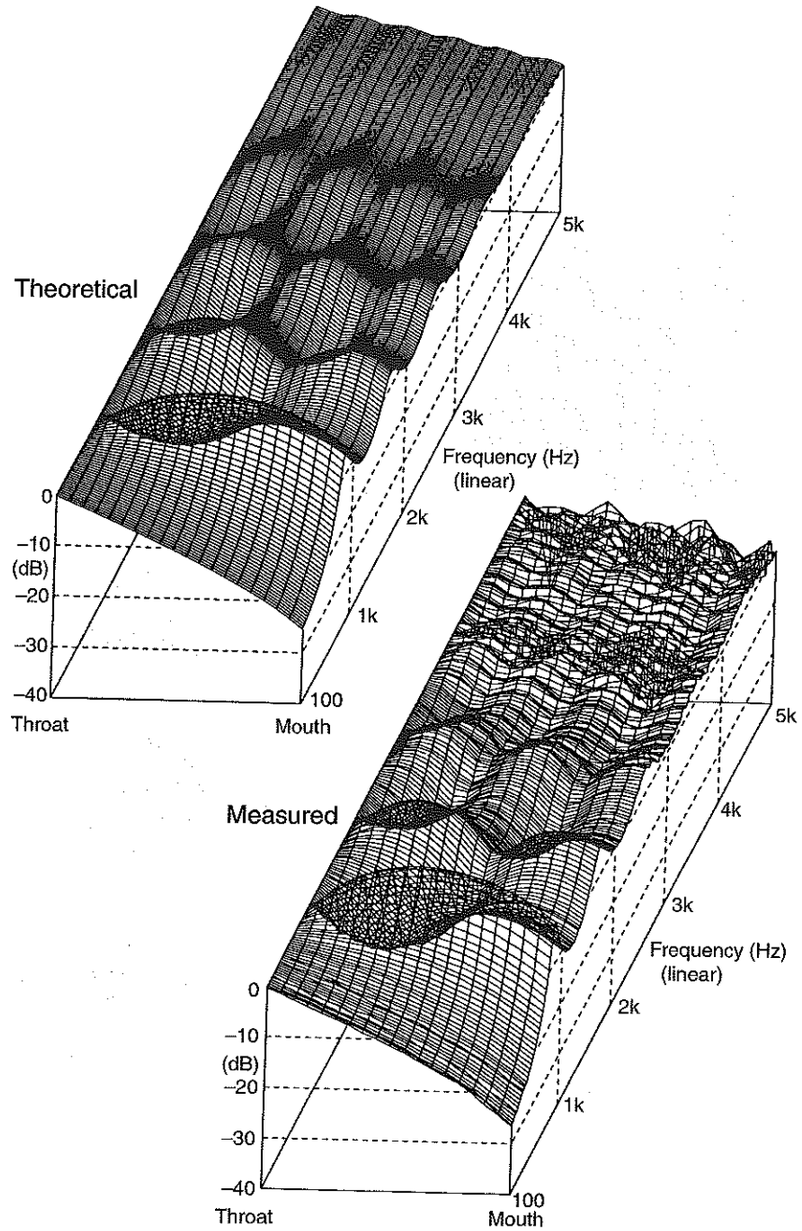

(a) Modulus of axial pressure distribution

Fig. 8.37 Comparison of theoretical and measured pressure distributions in the AX1 horn: (a) magnitude; (b) phase. Reproduced with permission from reference [8.7]. (*Continued overleaf.*)

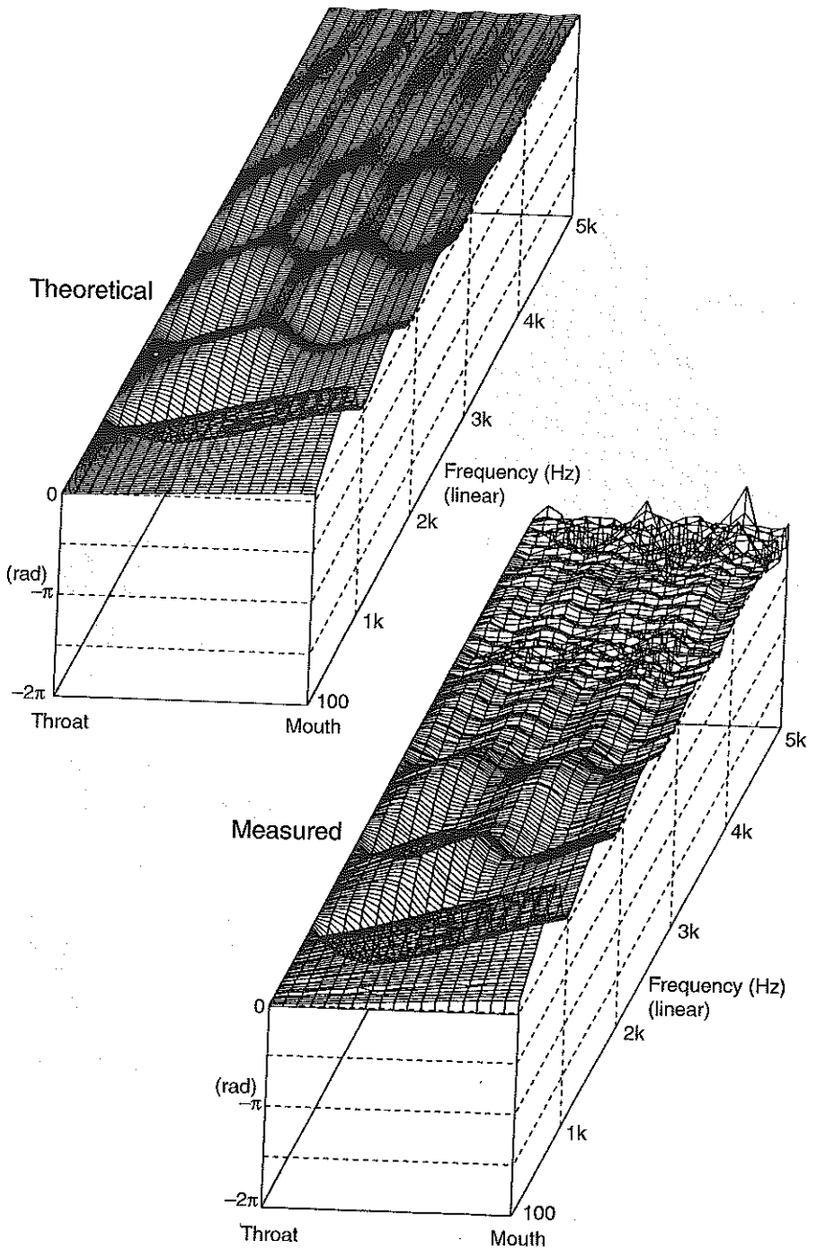

(b) Phase of axial pressure distribution

Fig. 8.37 (*continued*)

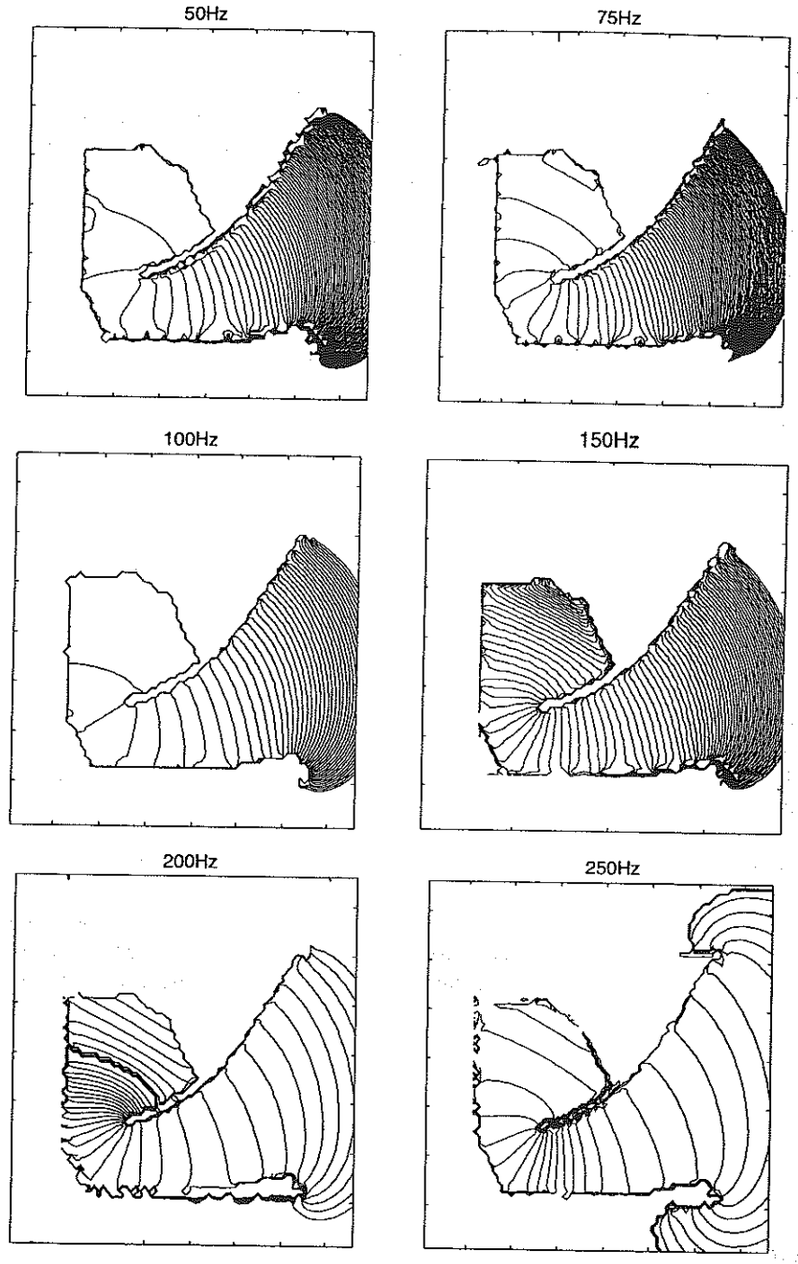

Fig. 8.38 Theoretical wavefronts in a 'bass bin'. Reproduced with permission from reference [8.8].

Fig. 8.36, together with curves of the transmission coefficient. This is a measure of the sound power relative to that generated in an anechoically terminated tube of the same cross-sectional area as the throat. It will be seen that, except for the conical horn, for which the specific acoustic radiation impedance is given by Eq. (6.25), the impedance becomes imaginary below a cut-off frequency, and power radiation is impossible. Practical horns are not infinitely long, and some degree of wave reflection from the mouth cannot be avoided. Figures 8.37(a) and (b) present a comparison between theoretical and measured forms of pressure field in an axisymmetric horn [8.7].

Commercially available horns assume a great variety of shapes that are designed to maximize output power and optimize directivity for particular applications, such as outdoor concerts or central clusters for auditoria. Their acoustic behaviour is analysed by the application of boundary element and/or finite element computer programs. An example of a boundary element method calculation of the wavefronts in a 'bass bin' is shown in Fig. 8.38 [8.8].

Questions

8.1 A point monopole source of volume velocity amplitude $Q_0 = 10^{-3}\,\mathrm{m^3\,s^{-1}}$ is situated in a rigid-walled duct of rectangular cross-section at a point $x_0 = 0.5a$, $y_0 = 0.6b$, where a and b are the dimensions of the cross-section. If $a = 0.5$ m and $b = 0.7$ m, and the duct is anechoically terminated at both ends, calculate the sound power of the source at 400 Hz. [Hint: either use $W = \mathrm{Re}\{\tilde{Q}\tilde{p}^*\}/2$, where p is the sum of the propagating mode pressures, or integrate the axial component of intensity over any cross-sections on both sides of the source.]

8.2 The duct specified in the previous question is lined with a locally reactive sound-absorbent material with a normal specific acoustic impedance ratio $z'_n = 4.0$ (any reactive component has been neglected in order to simplify the calculations). Calculate the axial attenuation rate of the principal mode at 100 Hz and 1 kHz.

8.3 A rigid piston of mass M slides freely in a tube of radius a that is terminated at a distance l by a rigid plug containing a small hole. The acoustic impedance of the hole is assumed to be purely resistive. Derive expressions for the mechanical impedance presented to an external force acting on the piston and the flow rate through the hole when the piston is excited by a harmonic force of unit amplitude. Identify any conditions of resonance. Assume that the piston does not leak flow around its periphery.

8.4 Two opposed rigid steel pistons of 300 mm diameter and 4 mm thickness are placed 35 mm apart in a tube within which they may slide freely. The pistons are mounted upon springs of stiffness $10^5\,\mathrm{N\,m^{-1}}$. The tube is anechoically terminated at each end. Determine the natural frequencies of the system. Assume that the pistons do not leak flow around their peripheries.

8.5 For the duct specified in Question 8.1 plot the axial phase and group speeds of the plane wave and of the (0,1) and (1,0) modes, against frequency. What are the asymptotic values of these speeds as the acoustic wavenumber tends to infinity?

8.6 A small loudspeaker in a rigid cabinet located in an anechoic chamber is excited by a short pulse of positive current followed immediately by an identical negative pulse. The open end of a long, anechoically terminated tube is placed symmetrically over the loudspeaker cone and the sound pressure–time history is recorded. The tube is then removed and the pressure–time history recorded at the same position. Sketch the sound pressure–time histories in the two cases on the basis of the assumption that the motion of the loudspeaker cone is controlled by its inertia. [Hint: Consider Eq. (6.23) and z of a plane wave.] In qualitative terms, what effect do you think the stiffness and damping of the loudspeaker system and the inductance of the voice coil would have on the pressure–time history if the same time history of voltage were applied to the loudspeaker? [Try this experiment in the lab.]

8.7 Prove that the functions $\cos(m\pi x/l)$ and $\cos(n\pi x/l)$ are orthogonal over the interval l.

8.8 Two identical side branch filters are attached to a tube at a separation distance l. The tube is anechoically terminated beyond the second filter. Derive an expression for the acoustic impedance ratio at the entrance to the junction with the first filter as a function of kd. [Hints: Represent the acoustic impedance ratio of the side branch simply as Z'_b. Use the impedance transfer expression in Eq. (4.22), with appropriate substitution of Z' for z', to express Z'_1 for the filter first encountered by the incident wave as a function of kl and Z'_2 at the junction with the second filter.] Consider the result at frequencies for which $kl = \pi$ and $kl = \pi/2$. Interpret your results in terms of the influence of the second filter on the impedance downstream of the joint with the first filter. Have the results got significance for practical noise control?

8.9 Derive expressions for the sound power transmission coefficient of a short ($kl \ll 1$) area constriction in an otherwise uniform duct in terms of the two-port formulation and the transfer impedance formulation. If they don't give the same result, something's wrong.

8.10 Repeat the analysis of Section 8.7.1 for a duct with pressure release ($z_n = 0$) walls. Sketch the modal pressure distributions across the duct for the lowest three modes. How do the modal cut-off frequencies compare with those of the rigid-walled duct of the same dimension? Consider the fate of a plane wave that travels along a rigid-walled duct and encounters a section of duct of the same cross-sectional dimensions, but with pressure release walls. What will happen below the lowest cut-off frequency of the duct with pressure release walls? [Hint: consider orthogonality.]

8.11 Derive Eq. (8.91).